Climate Impact Assessment of Sustainable Aviation Fuels

A scenario based assessment of the climate impact of sustainable aviation fuels in the year 2125

Pieter Koopdonk

Delft University of Technology

TU Delft

Climate Impact Assessment of Sustainable Aviation Fuels

A scenario based assessment of the climate impact of sustainable aviation fuels in the year 2125

by

Pieter Koopdonk

Student number:	4867866
Supervisor:	Dr. Feijia Yin
Graduating Professor:	Prof. Dr. Volker Grewe
Institution:	Delft University of Technology

TU Delft

Contents

Executive summary

This research reviews the challenges that aviation is facing to become more sustainable and discusses the role that sustainable aviation fuels could play. It investigates the impact that sustainable aviation fuels could have in reducing the climate impact of aviation. For this, the non-CO_2 emissions are also taken into account. The research question that lies at the basis of this report is formulated as follows: *How do different scenarios of usage of sustainable aviation fuels, impact the near surface temperature change due to aviation in the year 2125 compared to a baseline kerosene scenario?*.
The year 2125 is chosen to assess sustainable aviation fuel scenarios that start in 2025 with a time horizon of 100 years. By choosing such a large time horizon, this research looks further ahead then any other research on this subject.

Sustainable Aviation Fuel (SAF), which is a collective name for an alternative jet fuel made from renewable biomass or waste-based feedstock (bio-SAF), is found as one of the most viable alternative fuels. It can reduce the life cycle CO_2 emissions by up to 80%. The climate impact of contrails is also reduced as SAF emits fewer soot particles. Power-to-Liquid (PtL) is a special type of SAF as it is not made from biomass or waste feedstock, but uses hydrogen as the feedstock. PtL has the potential to reduce net CO_2 emissions by up to 100%.
The main challenge for bio-SAF is its limited scalability due to low availability of feedstocks. PtL does not suffer from this as it uses hydrogen as feedstock, but is much more expensive and not as technologically mature compared to bio-SAFs. The main advantage of SAF is that it can already be used in current aircraft and therefore requires no redesign.

The methodology that is used to answer the research question can be divided into three steps. The first step consists of the creation of the 3D emission inventory. This emission inventory is a 3D representation of the fuel and NO_x emissions due to aviation, as well as the flown distances. For this research, a baseline emission inventory is used that was calculated as part of the Master thesis of Rik Kroon [31]. This emission inventory is based on *flightradar24* data of 2019.
As a second step, this emission inventory must be adapted and reformatted such that it is compatible with the climate impact assessment model.
Finally, the adapted 3D emission inventory is used as input to the climate impact assessment model, along with a fuel consumption development, background emission development and a sustainable fuel scenario. It is chosen to use the climate impact assessment model AirClim [20] as it has been specifically developed to analyse the impact of aircraft technology. It is one of the more modern climate impact assessment models and has been developed by V. Grewe and A. Stenke (2008).

Two different SAF scenarios are compared to a baseline kerosene scenario. One scenario is based on EU legislation for the use of SAF named ReFuel EU (which starts to mandate a 1% SAF use from 2025), while the other is a SAF scenario where PtL does not reach a sufficient technological maturity. Additionally, a regional analysis is done to determine the region where the use of 1 kg of SAF achieves the highest reduction in temperature compared to the baseline kerosene scenario.

The simulations show that the use of SAF has a significant impact in reducing the climate impact of aviation. In 2125 the difference between the ReFuel EU SAF scenario and the baseline kerosene scenario is 57.03 mK, meaning a reduction in temperature change of 26.2%.
This scenario still surpasses the Paris Agreement goal of limiting the global temperature rise to 2.0 degrees Celsius by 61.0%. A Monte Carlo simulation shows that for only 6.9% (206 out of 3000 runs), this threshold is not exceeded. This research indicates that, for aviation to accomplish its relative contribution in accordance with the Paris Agreement, an initial overshoot of this goal is almost inevitable. Furthermore, this scenario relies on PtL, a SAF which uses hydrogen as feedstock and has not yet reached sufficient technological maturity. Without PtL the potential of SAF is reduced, as SAF made from biomass or waste feedstocks has limited scalability due to maximum feedstock availability. In a

scenario where PtL does not reach a sufficient technological maturity, the temperature change is only reduced by 26.60 mK (12.2%) compared to the baseline kerosene scenario.

These results show the importance of the non-CO_2 climate agents. Even with the significant use of SAF in the ReFuel EU scenario (resulting in a net 79% CO_2 reduction from 2070 onward), it exceeds the Paris Agreement goal by a significant margin. Especially the unaffected NO_x emissions hurt the climate impact gains that can be achieved.

The background emission scenario that is used for all non-aviation emissions also affects the results. A higher background emission scenario results in a smaller relative and absolute climate impact of aviation, due to the relatively lower aviation emissions when compared to the non-aviation emissions. For a lower background emission scenario the opposite is true. This impact is significant, as the difference in temperature in 2125 between the lowest and highest background emission scenario is 48.91 mK for the kerosene scenario.

The results of a Monte Carlo simulation with 3000 individual runs where 17 parameters were drawn for each run from a uniform distribution, show a large spread. This is a consequence of the large uncertainty ranges (up to $\pm$50%) from which the parameters were drawn. This result emphasises the large uncertainties that are associated with the climate impact of aviation.

Finally, a regional analysis is done to determine the region where the use of 1 kg of SAF has the highest reduction in temperature compared to the baseline kerosene scenario. The results of this analysis show that 1 kg of SAF can best be used in the South and Middle America region, as it leads to the greatest reduction in temperature. This same result is obtained when each region has their own individual growth rate for Revenue Passenger Kilometer (RPK).

This research has led to a number of recommendations for future studies.
It is found that some discrepancies in the results compared to other studies could be contributed to the emission inventory. It would be advisable to do the same simulations and analyses with emission inventories from similar studies.
This report only focuses on the use of SAF as an alternative aviation fuel, but also discusses the potential that liquid hydrogen can have to reduce the climate impact of aviation. A recommendation for further research is to also incorporate liquid hydrogen in these simulations.
For the regional analysis it was discovered during verification that the contrail model is not entirely valid on a regional scale when assessing the climate impact of contrails. This should be addressed for future research.
The regional analysis gives a good indication of how the use of 1 kg of SAF can be optimised and answers the initial question that led to the analysis. However it does not lead to the most optimal SAF usage. This is achieved by specifically identifying high contrail impact flights and ensuring that these flights use the maximum amount of SAF. Further research can be done to identify these specific flights to optimise the use of the limited amount of SAF.

Nomenclature

Abbreviation	Definition	Unit
ADS-B	Automatic Dependent Surveillance–Broadcast	
ATAG	Air Transport Action Group	
CORSIA	Carbon Offsetting and Reduction Scheme for International Aviation	
CST	Clean Skies for Tomorrow	
DAC	Direct Air Capture	
EI	Emission Index	
ERF	Effective Radiative Forcing	mWm^{-2}
GHG	Greenhouse Gas	
GWP	Global Warming Potential	
ICAO	International Civil Aviation Organization	
IPCC	Intergovernmental Panel on Climate Change	
IATA	International Air Transport Association	
nvPM	non-volatile Particulate Matter	
PMO	Primary Mode Ozone	
PtL	Power-to-Liquid	
RF	Radiative Forcing	mWm^{-2}
RPK	Revenue Passenger Kilometer	
SAF	Sustainable Aviation Fuel	
SSP	Shared Socioeconomic Pathway	
UHC	Unburned Hydrocarbons	

List of Figures

List of Tables

Introduction

Aviation has become an integral part of our modern society, connecting people and businesses around the world. However, the aviation industry is facing increasing pressure to reduce its environmental impact, particularly in terms of carbon emissions. Aviation has contributed to approximately 5% [32] of all anthropogenic climate change. At the current rate, the carbon emissions of aviation are forecast to double by 2050 [4].
The aviation industry is considered one of the 'hard to decarbonize'-sectors, which would increase the relative carbon footprint of aviation significantly by 2050 [34]. The ICAO (International Civil Aviation Organization) has therefore introduced the Carbon Offsetting and Reduction Scheme for International Aviation (CORSIA) [25]. This aims to achieve net-zero growth of CO_2 emissions from 2020 onward. Due to the COVID pandemic this has been achieved so far, however the effect of this measure is hard to estimate. With that being said, in 2022 aviation has already reached 80% of the pre-pandemic level of carbon emissions [27].
As a result, there is a growing need for sustainable aviation fuels that can reduce carbon emissions. However, an underrepresented issue is that of the non-CO_2 emissions, as these are estimated to account for approximately 2/3 of the climate impact of aviation [33].

This research will review the challenges that aviation is facing to become more sustainable and discuss the role that sustainable aviation fuels could play. It will investigate the impact that sustainable aviation fuels could have in reducing the climate impact of aviation. For this, the non-CO_2 emissions will also be taken into account. The research question that lies at the basis of this report is formulated as follows: *How do different scenarios of usage of sustainable aviation fuels, impact the near surface temperature change due to aviation in the year 2125 compared to a baseline kerosene scenario?*.
The year 2125 is chosen to assess sustainable aviation fuel scenarios that start in 2025 with a time horizon of 100 years. By choosing such a large time horizon, this research looks further ahead then any other research on this subject. This question is further divided into the following four sub-questions, which will be discussed in this report:

- How does current aviation affect climate change?
- What are the most viable alternative aviation fuels?
- What are the most viable alternative aviation fuel scenarios?
- How do the uncertainties that are associated with the climate impact of aviation affect the results?

Each of these sub-questions will contribute essential knowledge that is required to answer the research question.

This report will be structured as follows. Chapter 1 discusses the theoretical knowledge that is essential for this research. This includes the different emission species which are emitted during flight and how the fuel consumption of aviation has developed. Sustainable alternative aviation fuels will also be discussed in this chapter. The first three sub-questions will be addressed here. Chapter 2 will walk through the steps that will lead to the results. The creation and adaptation of the emission inventory will be presented, and the climate impact assessment model will be explained. All the different analyses and simulation set-ups will also be discussed here. The results of the simulations and the discussion of these results will be presented in Chapter 3. Finally, the report concludes with a summary of the most important findings and an answer to the research question and recommendations for future research will be given.

1 Theoretical Background

This chapter lays the theoretical foundation for understanding the climate impact of aviation and the potential of sustainable alternative aviation fuels. Section 1.1 discusses the emissions of conventional kerosene-powered aviation. This is followed by Section 1.2, which shows how the aviation fuel burn has developed in the past. Section 1.3 and Section 1.4 discusses the viable and nonviable sustainable alternative aviation fuels. Finally, Section 1.5 presents some future scenarios from previous studies that use these alternative fuels.

1.1. Aviation emissions

To gain an understanding of the climate impact of aviation, one must understand the input and output of the combustion process of an aircraft engine. This is presented in Figure 1.1.

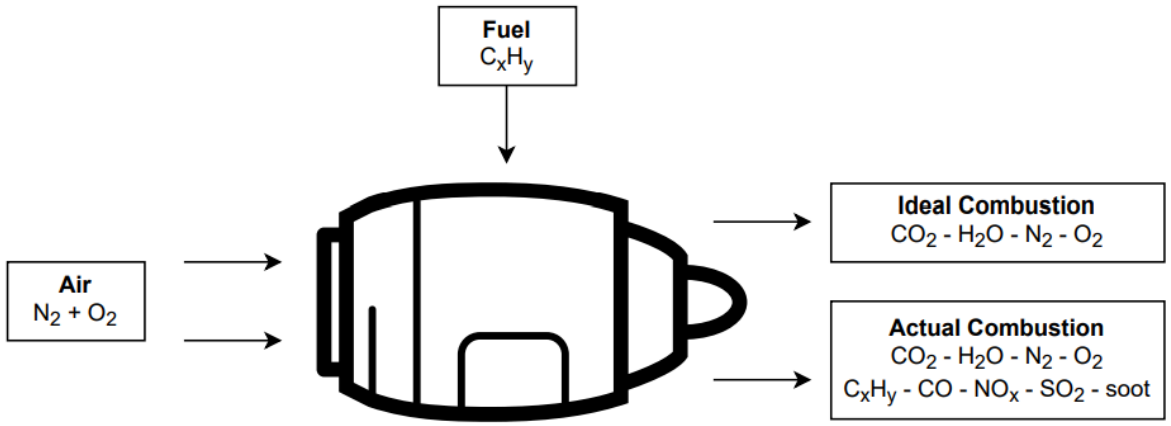

Figure 1.1: The chemical combustion products when using a hydrocarbon fuel such as kerosene [15].

A hydrocarbon fuel is mixed with the air and burned inside the engine. CO_2 and H_2O are products of complete combustion, while CO, soot and unburned hydrocarbons (UHC) are products of incomplete combustion. Additionally, NO_x is a byproduct of combustion and SO_x is a result of sulfur fuel impurities. Each of these combustion products will be discussed in more detail below.

CO_2 is the most well known greenhouse gas (GHG). Equation 1.1 shows the chemical equation of complete combustion, through which CO_2 is formed.

$$\mathrm{C}_x\mathrm{H}_y + a\,(\mathrm{O}_2 + z\ \mathrm{N}_2) \rightarrow x\mathrm{CO}_2 + \frac{y}{2}\mathrm{H}_2\mathrm{O} + a \cdot z\ \mathrm{N}_2 \tag{1.1}$$

Hydrocarbons can have a variety of different chemical compositions as indicated by x and y. The chemical formula for kerosene is typically between $C_{12}H_{26}$ and $C_{15}H_{32}$. With Equation 1.1 it can be calculated that approximately 3.15 kg of CO_2 is formed for each kilogram of kerosene. CO_2 is a GHG with an atmospheric lifetime of centuries, meaning that it will stay in the atmosphere for a long time and continue to have an affect on Earth's temperature long after it has been emitted. CO_2 contributes to approximately 32% of all Effective Radiative Forcing (ERF) of aviation [33]. Radiative Forcing is a metric that is used to relate emissions to their climate impact. Since the CO_2 emission from a flight are

directly related to the fuel burn, fuel efficiency improvements will reduce these emissions.

H_2O is another GHG. Similarly to CO_2, its emission is directly related to the fuel burn and can be calculated to be 1.23 kg per kilogram of kerosene. The direct greenhouse impact of H_2O is relatively small (approximately 2% of the ERF [33]), however it does contribute to the formation of contrails, which will be discussed further on. The reason for this relatively low climate impact is the short lifetime of H_2O in the atmosphere (lifetime of days). However, there is an important altitude effect regarding the lifespan of H_2O. The lifespan of H_2O increases with altitude, up to 4.4 years at 35 km altitude [39]. This significantly increases the ERF of H_2O the higher it is emitted.

CO can be considered as a very weak GHG and its direct impact is negligible. However, it does react with O_2 to form CO_2 in the troposphere. Incomplete combustion occurs most frequently at idle engine conditions, so not actually during flight. The emission rate is very low, and its impact on climate change is insignificant [15].

Similar to CO, UHC is a product of incomplete combustion meaning that its emission is maximised at idle engine conditions. Its climate impact is also negligible.

Soot is also a product of incomplete combustion, however soot is not as well understood as some of the other emission species. On the contrary to CO and UHC, soot emissions are maximised at maximum thrust conditions. The formation of soot is related to the aromatic content of the fuel. More energy is required to break the chemical bonds and oxidize the aromatic rings compared to hydrocarbon chains. The hydrogen to carbon ratio (H:C) is lower for aromatic molecules, meaning that the H:C ratio is a good predictor for the amount of soot that is emitted for a fuel [44]. The direct climate impact of soot is estimated at 0.1-4.0% of the total ERF, meaning that is does not have a huge impact. However, the number of soot particles plays an important role in the climate impact of contrails, which does account for a significant part of the ERF of aviation. Contrails will be discussed further down below.

NO_x emissions (which includes NO and NO_2) depend on the combustion temperature, pressure and the mass flow [5]. The climate impact of NO_x is not as straightforward as some of the other emission species, as NO_x is an indirect GHG. The emission of NO_x results in the production of the GHG ozone (O_3) through photochemical reactions. Ozone has a lifetime of 100-200 days and the impact of these emissions are limited to a regional scale [17]. This is the short-term effect of NO_x emissions. There is also a long-term cooling effect: the NO_x emissions lead to a destruction of methane (CH_4, a GHG which is more than 20 times stronger than CO_2), which in turn also reduces the O_3 and H_2O concentrations. This long-term reduction in O_3 is called Primary Mode Ozone (PMO). The lifetime of CH_4 is 9-12 years, meaning that this cooling effect takes much longer compared to the short-term effect of the increase in ozone. In total the ERF as a result of the NO_x emissions are estimated at approximately 18% of the total ERF from aviation, but it is important to make a distinction between the short-term warming effect and the long-term cooling effect. The short-term increase in ozone is estimated to have an ERF of 49.3 mWm^{-2} (compared to 34.3 mWm^{-2} for CO_2 for example). The total long-term cooling effect is estimated at -35.0 mWm^{-2} [33]. It must be noted however that recent studies have indicated that the total RF of NO_x is underestimated [19], so the climate impact is likely higher. The climate impact of NO_x emissions is also dependent on the altitude; NO_x emissions at 10-12 km altitude have a larger climate impact. NO_x emissions at the surface actually have a net cooling effect [40].
Reducing the NO_x emissions is not so trivial without compromise, as this is mainly done by lowering the combustion temperature. On the contrary however, fuel efficiency improvements are mainly a result of higher combustion temperatures [5]. A recent study suggests that reducing NO_x emissions by sacrificing fuel efficiency may not be beneficial for the climate impact of aviation [40]. Other methods to decrease NO_x emissions without sacrificing fuel efficiency are under development.

SO_x emissions are a result of sulfur impurities in the fuel that mix with oxygen. These emissions are the highest at maximum thrust conditions, similar to soot. SO_x actually have a cooling effect due to their aerosol-radiation interactions, as they scatter incoming short-wave radiation [28]. This effect is estimated to be between -2.6 and -19.0 mWm^{-2} in ERF, with a best estimate of -7.4 mWm^{-2} [33]. SO_x also contributes to acid rain.

The final climate agent of aviation is that of contrails. Contrails are cloud-like lines of condensed water that are sometimes formed behind an aircraft. Whether contrails will form is dependent on certain atmospheric conditions and engine and fuel parameters, which is depicted by Equation 1.2. This equation shows the slope G of the exhaust mixing line; the higher the slope the greater the probability that persistent contrails will form. c_p is the specific heat of the air (constant pressure), P the ambient pressure, ϵ ratio of the molar mass of water to air, EI_{H_2O} is the emission index (EI) of water (kg of emitted water per kg of fuel), Q is the specific heat of the fuel and η is the propulsion efficiency.

$$G = \frac{c_p P}{\epsilon} \frac{EI_{H_2O}}{Q(1-\eta)} \tag{1.2}$$

In addition to these conditions, the atmospheric temperature must be low enough such that water droplets can freeze. At cruise level, this is at -38 degrees Celsius. Above this temperature, contrails will not form.
There are three different types of contrails that can be formed; non-persistent contrails, persistent contrails and cirrus contrails. A non-persistent contrail will disappear shortly after forming and has a negligible climate impact. A persistent contrail is a linear line behind the aircraft that can persist for hours, while a cirrus contrail is a contrail that will spread out (instead of maintaining a linear shape). The climate impact of contrails is determined by characteristics of the aerosol particles; this entails the number and the size of the ice crystals that the contrail consists of. As discussed previously, by reducing the aromatic content of aviation fuel, the number of formed soot particles is reduced by 50-70% [44]. This results in a reduction of the number of ice crystals and an increase in the ice crystal size. This will in turn reduce the ERF of contrails.
As contrail formation is dependent on atmospheric conditions, the probability of contrail formation is varying with altitude. This is shown in Figure 1.2. As can be determined from the figure, the largest probability of contrail formation is found at approximately 11 km altitude around the poles and 13 km altitude at the equator. These are the most likely locations for contrails to form, but it should be noted that in principle contrails could form at any location if the conditions are satisfied. This also means that these highest probability locations are not fixed and can change if the atmospheric conditions would change over time due to climate change for example.

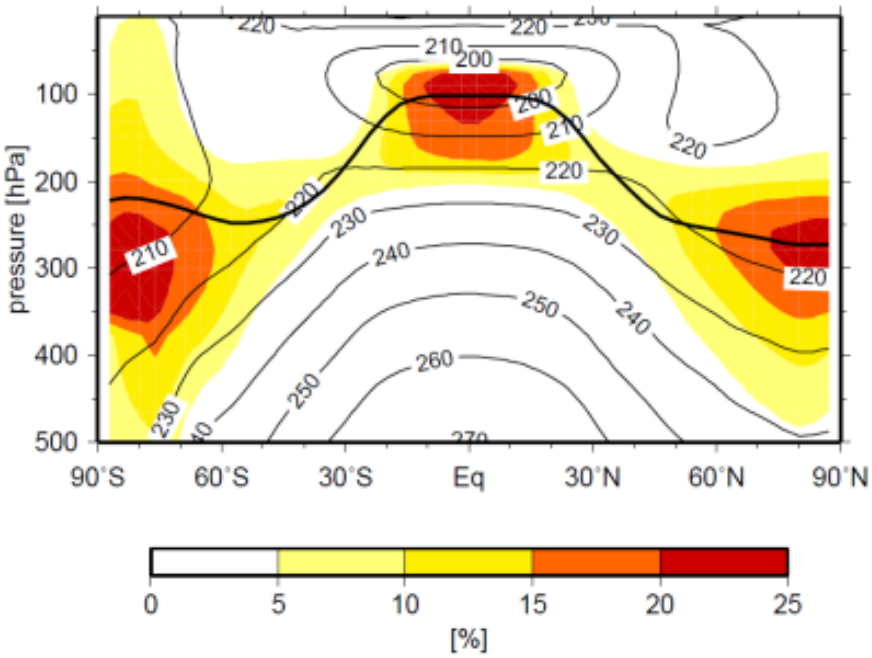

Figure 1.2: Persistent contrail formation probability with varying latitude and air pressure (altitude) [20].

The ERF of contrails is estimated at 57.4 mWm^{-2}. It should be noted that the uncertainty of the climate

impact of contrails is larger compared to that of some of the other climate agents. This is in part due to the fact that the climate impact of a contrail is very much dependent on the specific characteristics of the contrail and the time and location of the formation of the contrail. There are multiple sources of uncertainty in play here. First of all, the likelihood of a contrail forming at a certain location and time if an aircraft were to fly there introduces uncertainty. This refers back to Figure 1.2, where the formation of a persistent contrail is merely a matter of probability if the atmospheric conditions of that location at that time are unknown. The second source of uncertainty is related to how a persistent contrail would develop after forming. To accurately estimate the climate impact of a persistent contrail, its development and integration into the atmosphere would need to be modelled. There are many uncertainties related to this. For how long will the contrail continue to persist? Will it maintain its linear shape or will it develop into contrail cirrus? How will the contrail interact with other atmospheric features such as clouds? These questions show why the climate impact of contrail is so hard to estimate and is associated with so much uncertainty. This makes it much more difficult to model accurately compared to CO_2 for example.

In conclusion, there are six relevant climate agents (GHG) that cause the vast majority of climate change. These are CO_2, H_2O and contrails, while the NO_x emissions can be divided into the underlying climate agents CH_4, O_3 and PMO.

It is important to note that in the ICAO Carbon Offsetting and Reduction Scheme for International Aviation (CORSIA) [25], only the CO_2 emissions of aviation are accounted for. This is worrying as these emissions only contribute to approximately 1/3 of the ERF of aviation. However, in the hypothetical scenario that aviation would stop tomorrow, the climate impact of short lived climate agents would reduce quickly, while the climate impact of CO_2 would still contribute to warming for centuries.

An overview of how each climate agent contributes to climate change is shown in Figure 1.3, while the total climate impact and that of each individual climate agent is summarised in Figure 1.4.

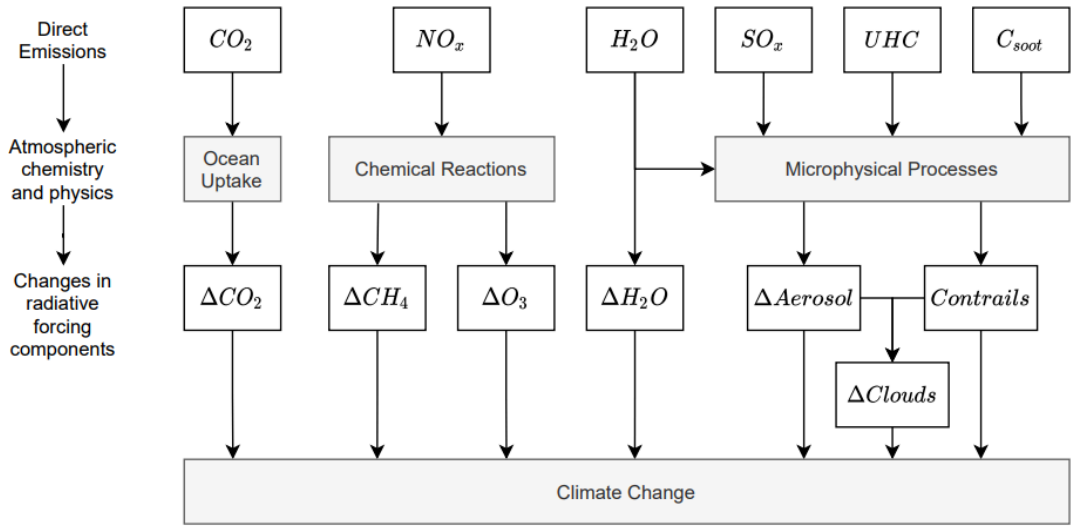

Figure 1.3: The contribution of each climate agent to climate change [15].

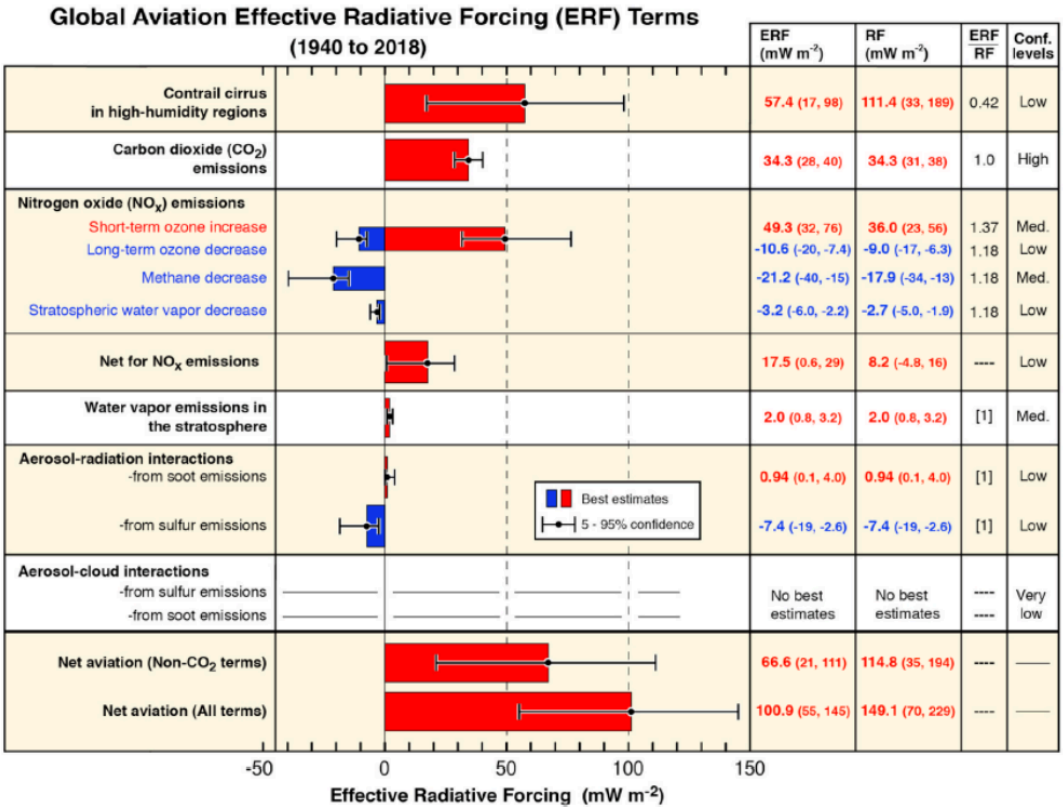

Figure 1.4: The Global Aviation Effective Radiative Forcing (ERF) for each climate agent from 1940 to 2018 [33].

1.2. Historical and future emission trends

Significant efficiency gains have been made since the beginning of commercial aviation, as is shown in Figure 1.5. The fuel burn of the aircraft that were introduced in 1960 was more than twice as high compared to the current generation of aircraft. These efficiency gains are a result of improved aerodynamic and engine efficiencies, lighter structures and more streamlined operations. However, due to the explosive rise in demand for aviation, the CO_2 emissions have grown rapidly despite these efficiency gains. This is apparent from Figure 1.6.

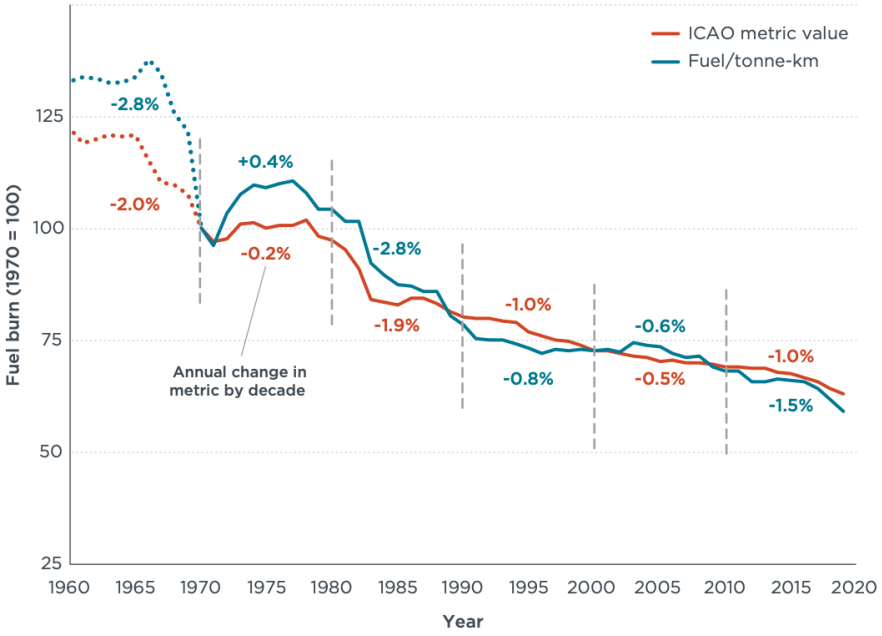

Figure 1.5: Aviation fuel burn trend from 1960 to 2020 [47].

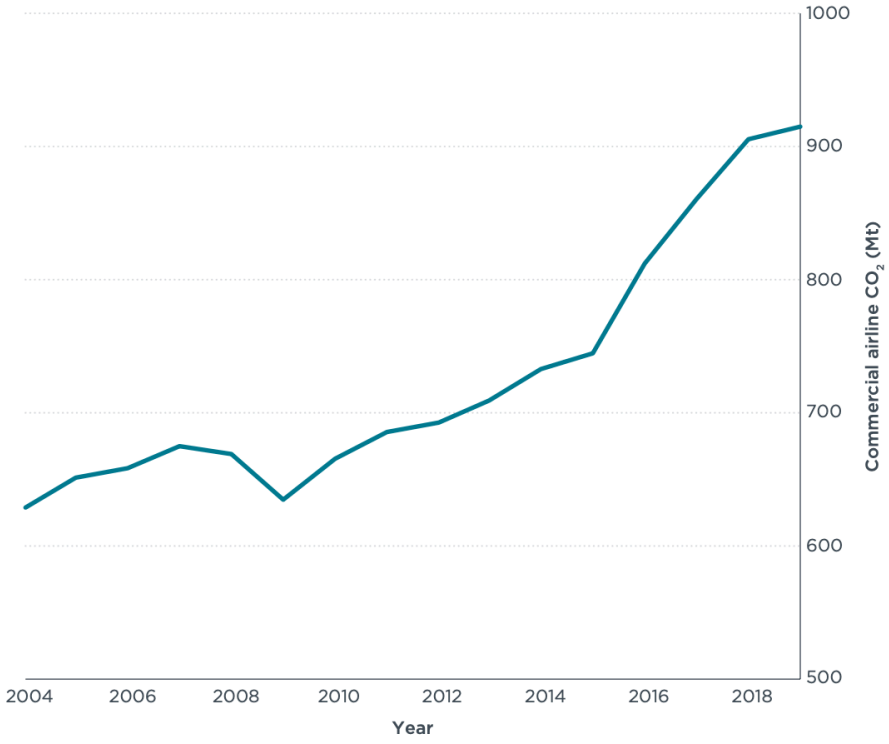

Figure 1.6: CO_2 emissions from commercial aviation between 2004 and 2018 [47].

Further efficiency gains are expected [13][47], but in combination with the forecast continuous growth in demand, a decrease in aviation emissions is not foreseen in the near future. On the contrary, emissions are forecast to have doubled by 2050, even with the expected efficiency improvements. As the emissions of other sectors are expected to decrease, the relative contribution of aviation to global warming is expected to have increased significantly by 2050 [4].

Therefore, it is clear that a change in direction is necessary if aviation wants to achieve its goal of net zero carbon emissions by 2050 to reduce its climate footprint. This is a necessity from an economic point of view as well, as it is not the question if, but when climate impact starts to be incorporated more into prices. With this, aviation would become increasingly expensive and out of reach for most people in the future. More sustainable alternative aviation fuels can play a large role in this necessary change of direction, to replace the unsustainable use of kerosene. These will be discussed in the next section.

1.3. Viable alternative aviation fuels

Multiple studies have indicated various promising routes for zero emission by 2050 using sustainable alternative fuels [4][23][45]. These alternative fuels will be discussed in the next section.

1.3.1. Sustainable Aviation Fuel

Sustainable Aviation Fuel (SAF) is a collective name for an alternative jet fuel that is made from renewable biomass or waste-based feedstock. This ensures that it has a lower carbon life cycle compared to conventional jet fuel, and often these feedstocks are already present in or would otherwise release back into the atmosphere. A special type of SAF is Power-to-Liquid (PtL) as this fuel is not made from biomass or waste feedstock, but is produced by splitting hydrogen in a process called electrolysis. The required carbon is often extracted from the atmosphere or from industrial waste gas. There are many different types of SAF and as of the moment of writing, 9 conversion processes for SAF production have been approved [26]. SAF is currently considered a drop-in fuel to be mixed with conventional jet fuel. The different conversion processes for SAF production have different blending limits, but most are approved for blending up to 50%. Work is ongoing to reach 100% [35]. A huge benefit of SAF is that it can be blended with conventional jet fuel without any alteration to the engine or aircraft. Already SAF is added to flights, however less than 1% of total jet fuel demand consists of SAF currently [24]. The SAF blends are compatible with current fuel delivery and airport fuelling infrastructure.
The emissions during flight are very similar for SAF compared to conventional kerosene. The main difference is that SAF emits fewer soot particles [2], which reduces the climate impact of contrails [44]. This effect is significantly more substantial for pure SAF-powered aircraft compared to mixes with kerosene [30]. The life cycle CO_2 emissions can be up to 80% lower for pure SAF, with blends of 50% leading to a reduction of 40% [45].

Bio-SAFs

Bio-SAFs are made from many different feedstocks, which are shown in Figure 1.7.

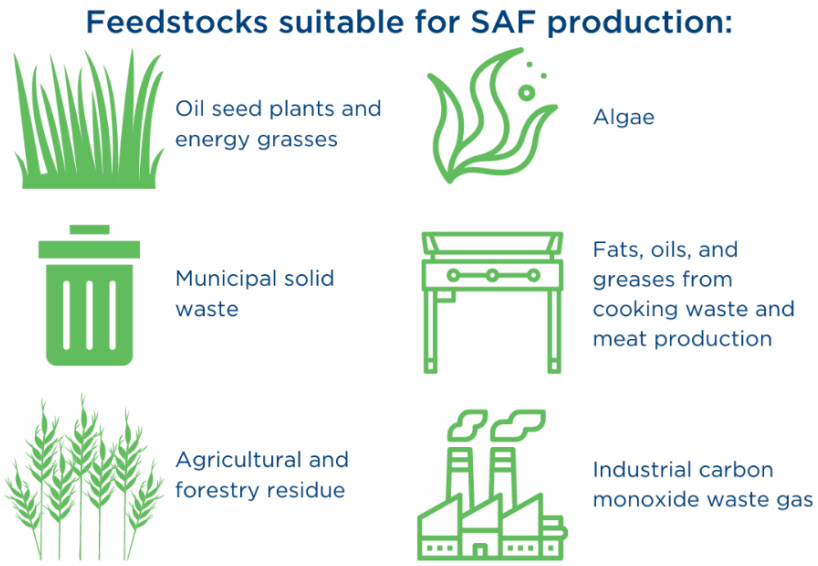

Figure 1.7: Suitable feedstocks for Sustainable Aviation Fuel (SAF) production [38].

There are large differences between the various feedstocks when it comes to how sustainable they are and their GHG emission reduction. Edible oil crops and sugars (such as palm, soybean or sugarcane) are not sustainable feedstocks and would not lead to substantial GHG emission reductions. These would actually be taking up valuable land and would be competing with other crops. More sustainable feedstocks are therefore waste- and residue-based feedstocks. An important note here is that SAF production should not lead to a business case for other industries to produce carbon waste. Double-claiming emission reductions should also be avoided.
Growing non-food plant feedstocks for SAF production has additional potential benefits. These include the use of otherwise unproductive land, provide employment in rural areas and add revenue for farmers. When feedstocks are grown as cover crops in between growing seasons, it can also enrich the soil for conventional crops [45].
The main challenge for bio-SAFs is the fact that the feedstocks are limited and this therefore limits the scale up potential. If the production of bio-SAF is optimised in terms of economies of scale and by ensuring availability of all viable feedstocks, it could supply 490 million metric tons of SAF per year. This is approximately the total estimated jet fuel demand in 2030 [35]. While this is a significant amount, it also means that bio-SAFs on its own are not a long-term solution when looking past 2030 towards 2050 and the late 21st century, when demand is estimated to be much higher. FlyZero [23] states that approximately only 20% of the SAF required to power the global fleet by 2040 is expected to come from bio-SAFs. Additionally, bio-SAFs are also competing with renewable diesel (used for road transport) for feedstocks.

Power-to-Liquid
PtL can be a solution to the problem of limited scalability of bio-SAFs, as PtL uses hydrogen as the feedstock. PtL is not as mature as some of the other SAF production pathways, as the first industrial-scale production facility using Direct Air Capture (DAC) is only planned for 2026 [7]. Direct Air Capture is essential for PtL as the required carbon to produce PtL will directly be extracted from the atmosphere, resulting in net CO_2 emission reductions of up to 100% [34]. The major drawbacks of PtL are the high cost compared to other SAFs and the fact that is an inefficient method of using hydrogen, compared to liquid hydrogen propulsion. Regarding this latter drawback, the production of PtL requires 45% more renewable energy and 22% more hydrogen compared to the production of liquid hydrogen [23]. This means that the cost of PtL will become uncompetitive compared to liquid hydrogen propulsion when both scale up and become more mature. However, as mentioned previously, liquid hydrogen requires major redesigns for aircraft and infrastructure while PtL is compatible with current aircraft and engines. Since PtL requires a high amount of renewable energy to be produced compared to bio-SAFs and requires DAC, which is currently not mature and very expensive, its costs are much higher also compared to bio-SAF. Clean Skies for Tomorrow [34] therefore defines three milestones that need to be achieved for PtL commercialisation: renewable energy cost reductions of 30%, electrolyzer technology cost reductions of 50% and efficient DAC with cost reductions of 50-80%. ATAG (Air Transport Action Group) [45] expects PtL to account for 42-57% of total SAF production by 2050. With technologies maturing, production processes becoming more efficient and more scalable, and with carbon taxed kerosene, the expectation is that bio-SAFs and liquid hydrogen could already become cheaper than kerosene in the early to mid 2030s respectively [23][35]. A sufficient carbon tax on kerosene is necessary for this.

1.3.2. Liquid hydrogen

Liquid hydrogen is considered a viable alternative fuel for aviation due to its high specific energy and zero carbon emissions. The specific energy is three times higher compared to that of kerosene. This makes it a promising candidate from a payload-range standpoint. However, specific energy does not tell the whole story as the volumetric energy density of liquid hydrogen is four times lower compared to kerosene. This means that a big tank is required to store the liquid hydrogen on board, much larger than what is currently used for kerosene. This will require a redesign of aircraft to accommodate the storage tank. This will negatively impact the aerodynamic performance. Additionally, liquid hydrogen has a boiling point of 20 K, meaning that the tank would have to be very well insulated to ensure the hydrogen remains in a liquid state. This would not be a problem for gaseous hydrogen, however this would need to be stored at a pressure of 700 bar to achieve a somewhat viable density. In this case, the required wall thickness for the storage tank would increase the mass of the storage tank significantly.

This would further negatively impact the payload-range diagram compared to liquid hydrogen [4].
There are two different types of propulsion methods involving liquid hydrogen that could be viable: gas turbine propulsion and fuel cell propulsion.

Gas turbine propulsion
For gas turbine propulsion, the hydrogen is simply burned in the gas turbine as a fuel. The liquid hydrogen from the tank will need to be delivered to the combustion chamber at high temperature and pressure, such that the hydrogen fuel is delivered in a supercritical state [46]. Using liquid hydrogen as a fuel completely eliminates CO_2 emissions. The NO_x emissions are estimated to be reduced by 50-80%. This is due to the fact that hydrogen can be burned with leaner combustion, resulting in a lower combustion temperature. Additionally, higher burning velocities allow for higher rates of reaction and mixing, which ensures that the hydrogen stays in the combustion chamber for a shorter time. This also reduces NO_x emissions [4]. On the contrary, the H_2O emissions would be 2.6 times as high. The low lifetime of H_2O ensures that the climate impact increase that this has is of an order of magnitude lower compared to that of the other emission reductions.
Finally, the climate impact from contrails is expected to decrease. There are large uncertainties surrounding this however. The thought process is that the additional water emissions from the hydrogen combustion leads to more contrail formation, but that these contrails are likely to be optically thinner and less persistent (due to the lack of soot emissions). This would mean that the overall climate impact of contrails is reduced [46]. This is also confirmed by the first simulations [29], but flight tests and further research is necessary to validate this.

Fuel cell propulsion
For fuel cell propulsion, the liquid hydrogen needs to be delivered from the tank to the fuel cell at low pressures of around 1-2 bar. The hydrogen must also be in a gaseous state and at room temperature. Therefore, the liquid hydrogen must be passed through a heat exchanger to be warmed to approximately 300 K [46]. Like hydrogen gas turbine propulsion, fuel cell propulsion will also have no CO_2 emissions, but it will additionally also have no NO_x emissions. H_2O emissions are again 2.6 times higher compared to kerosene. The climate impact of contrails is similar to that of hydrogen gas turbine propulsion, but has the potential to be lower due to the possibility that the water vapour from the fuel cells can be collected [4]. A downside of fuel cell propulsion is that the outright performance is not as good as that of gas turbine propulsion due to the lower power density, meaning that it weighs more for the same amount of power. This means that fuel cell propulsion would only be viable for short-range aircraft [23].

Challenges and limitations of liquid hydrogen
There are many technological challenges for which a solution needs to be found to make liquid hydrogen a viable alternative aviation fuel [4][45]. These involve challenges surrounding the cryogenic storage systems, such as good insulation for the entire fuel system to minimize boil-off and to protect against surface frost or air liquefaction. These form serious safety hazards.
Additionally, there are many infrastructural challenges as well. A refuelling system would need to be found that enables similar flow rates compared to kerosene. In the early phases with low demand, existing infrastructure can be used to distribute the liquid hydrogen to various airports via trucks, however during further scale-up, this will not be sufficient.
Furthermore, handling and safety regulation would need to be developed for liquid hydrogen in aviation, as the characteristics are vastly different to that of conventional jet fuel. FlyZero [23] defines six fundamental technology bricks which need to be developed further to enable liquid hydrogen aviation. These are related to the Hydrogen Gas Turbines & Thrust Generation, Fuel Cells, Electrical Propulsion System, Thermal Management, Cryogenic Hydrogen Fuel System & Storage and Aerodynamic Structures.
Solutions to many of the above mentioned challenges are set to be found in the next 2-7 years according to industry experts [4]. Airbus has even announced that it plans to bring a zero-emission aircraft into service by 2035 that is equipped with a hydrogen-powered fuel cell engine [1].
A serious concern for liquid hydrogen is the potential leakage. As hydrogen is the smallest molecule, it can easily pass through materials. This can pose a safety concern as hydrogen is highly flammable.

This can be mitigated by the previously mentioned insulation for the entire fuel system. However another aspect of hydrogen leakage is that of its climate impact. Hydrogen is an indirect GHG as it effectively increases the atmospheric lifetime of methane, ozone and water vapour by reacting with OH in the atmosphere [10]. The hydrogen leakage rate is estimated to be between 2.9% and 5.6% when considering the entire life cycle from production to transportation to end-usage [16]. It is estimated that every 1% of hydrogen leakage rate has the RF of 0.5% of the fossil fuel system that it replaces [10]. This would mean that a 5% leakage rate results in the RF of 2.5% of the fossil fuel system total RF. From this it can be concluded that hydrogen leakage has a non-negligible climate impact, however this would still mean that switching to a hydrogen economy would significantly reduce the climate impact compared to a fossil fuel economy.
Finally, it is important to note that the liquid hydrogen must be produced with renewable energy to realise the aforementioned climate impact. Otherwise significant (CO_2) emissions will be released during production of the liquid hydrogen. This means that significant further investments are necessary to ensure enough renewable energy is available for the production of liquid hydrogen.
The discussed climate impact during flight of the alternative aviation fuels relative to kerosene is summarised in Table 1.1. This table gives the relative GWP (Global Warming Potential) values of each alternative fuel and climate agent compared to kerosene emissions. The large differences between the upper and lower limit values is explained by the uncertainties surrounding the climate impact of NO_x and contrails. The lower limit corresponds to a lower importance of NO_x, H_2O and contrails relative to CO_2 emissions while the upper limit corresponds to a relatively high importance of these climate agents relative to CO_2.

Average values	**CO_2**	**NO_x**	H_2O	**Contrails**	**Total**	**Lower limit**	**Upper limit**
Kerosene	100%	100%	10%	100%	**310**%	**205**%	**415**%
SAF	0%	100%	10%	75%	**185**%	**85**%	**300**%
H_2 turbine	0%	35%	25%	60%	**120**%	**50**%	**220**%
H_2 fuel cell	0%	0%	25%	30%	**55**%	**25**%	**100**%

Table 1.1: Relative Global Warming Potential (GWP) values due to in-flight emissions for each alternative fuel and climate agent compared to that of kerosene [4].

Finally, it is important to also assess the climate impact of these fuels during production. This is shown in Figure 1.8 for each of the discussed fuels with estimated 2030 production values, with a selection of five different bio-SAFs to illustrate the large differences in terms of their sustainability. Bio-SAFs from cover crops could potentially even have a negative climate impact for fuel production due to their ability to store carbon in the soil [29]. This figure further shows that selection of the more sustainable bio-SAFs is important to ensure a significant climate impact reduction, which in turn also emphasises the capacity limitations of bio-SAFs.

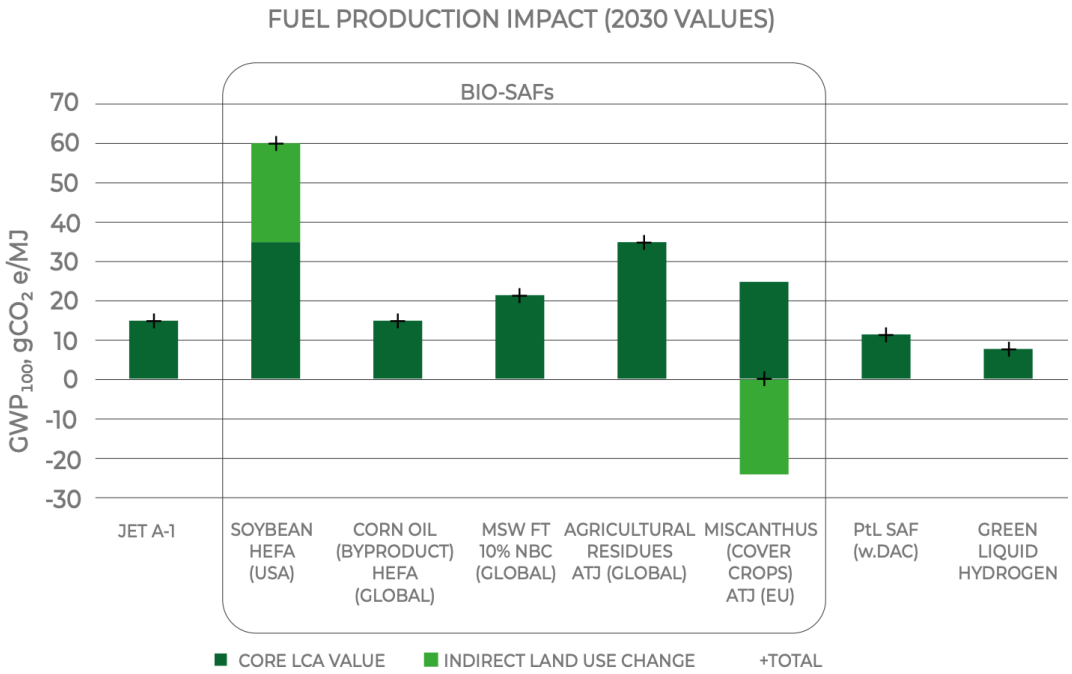

Figure 1.8: Estimated climate impact of fuel production in 2030 for each fuel, expressed in Global Warming Potential (GWP) with a 100 year time horizon [29].

1.4. Nonviable alternative aviation energy sources

Some of the less viable alternative energy sources will also be discussed briefly, with an explanation why these are not as viable compared to the previously presented alternative aviation fuels.

1.4.1. Battery Electric

From a sustainability perspective battery electric is the best form of propulsion, as it produces no in-flight emissions or air quality concerns. Additionally, the renewable electricity demand would be the lowest as the electricity can directly be used to charge the batteries, in contrast to the production of liquid hydrogen or PtL. However, current battery technology is insufficient to provide the performance that is needed for a reasonable range. A plane would need more than 50 kg of batteries to replace 1 kg of kerosene, resulting in a maximum range of 500-1000 km [35]. The outlook for further battery development is insufficient to warrant this a viable option. Furthermore, aircraft that fly using batteries do not loose weight during flight as is the case for other type of energy sources where the fuel burns off. This means that it is a less efficient manner of flying. Additional challenges are the vast amount of scarce raw materials that are required for batteries and the end-of-life considerations. Improvements in this area are being made, with the expectation that a strong supply chain will be established [46].
Battery electric could be viable in a hybrid set-up with SAF or liquid hydrogen gas turbine propulsion as this removes some of the performance related concerns. However hybrid set-ups will not be considered in the scope of this research, as the aim is to assess the impact of each alternative aviation fuel. This is best done by excluding hybrid set-ups. This also includes a hybrid set-up with hydrogen fuel cell and hydrogen gas turbine propulsion.

1.4.2. Ammonia

The last assessed alternative aviation fuel is that of ammonia. Advantages of ammonia over hydrogen are in the fact that ammonia can be stored at much higher temperatures (240 K vs 20 K) and has a much higher density (682 kgm^-3 vs 71 kgm^-3). These combined would mean that the total volume that would need to be taken on board would be much lower and that the insulation would not lead to such a big increase in mass. This means ammonia might even be stored in the wings similar to kerosene and a redesign of aircraft would not be as drastic. However, using ammonia as fuel also introduces other complexities. Before ammonia can be used to power a gas turbine or fuel cell, it needs

to be cracked (meaning that ammonia is decomposed into hydrogen and nitrogen). For a fuel cell the ammonia needs to be cracked for 100% before it is delivered to the fuel cell. For gas turbine combustion approximately 30% is necessary [46]. Lightweight cracking technology is currently being pursued, but presents both a mass and operational challenge. However, the main drawback for ammonia comes from the significantly higher NO_x emissions due to the nitrogen content in ammonia. This leads to an unacceptable increase in NO_x emissions and poses further local air quality concerns. Additionally, ammonia is toxic and corrosive.

1.5. Future alternative aviation fuel scenarios

There are multiple recent in-depth studies that have looked at how to make the aviation sector more sustainable. These studies all present different scenarios on how the aviation sector should reach net zero carbon aviation in 2050.

FlyZero [23] has developed three liquid hydrogen aircraft concepts. The regional concept can carry 75 passengers and has a range of up to 800 nautical miles (nmi). This is slightly under 1500 km. This concept is powered by a hydrogen fuel cell system. The second concept is that of a narrowbody aircraft that can carry 179 passengers with a range of 2400 nmi (4445 km). This aircraft would be powered by hydrogen gas turbines. Finally, the midsize concept can carry 279 passengers for up to 5750 nmi (10649 km). With this range, the aircraft is able to efficiently serve 93% of currently scheduled long haul flights. This aircraft would also be powered by hydrogen gas turbines. It is important to note that, because of the long lifetime of aircraft of approximately 30 years, there is only one more cycle of fleet renewal for airlines before 2050. This means that there is only one opportunity before 2050 to introduce a hydrogen aircraft, and this will be around mid-2030.

Two possible scenarios to introduce these aircraft onto the market are suggested [22]. The first scenario is to start with the midsize aircraft concept with an introduction in the early- to mid-2030s. Up until this point, bio-SAFs need to be rapidly rolled out through the 2020s and 2030s. PtL would only play a small role when capacity constraints of feedstocks for bio-SAFs would need to be supplemented by PtL. The narrowbody aircraft would then be introduced shortly after the midsize aircraft (late-2030s), with the regional aircraft being introduced in the early-2040s. Since the midsize aircraft can serve the greatest market of the three concepts, starting with this aircraft ensures that liquid hydrogen can play a great role in the fuel mix early on, meaning that the requirement for SAF is relatively limited. Another advantage lies in the fact that smaller infrastructure investments would be necessary early on, as a relatively small number of airports can serve as hydrogen hubs due to the greater relative range of the midsize aircraft concept. Fuel tankering could even be an option, due to the higher mass energy density of hydrogen compared to kerosene. Because of this, the narrowbody concept for example would only suffer from a 1.3% fuel consumption penalty on the outbound leg of a 1000 nmi round trip compared to 6.3% for a kerosene-powered A320neo [9]. This would allow early hydrogen aircraft to fly to airports without hydrogen re-fuelling infrastructure.

The second scenario consists of first introducing the regional aircraft in the mid-2030s. As in the first scenario, bio-SAFs are rolled out rapidly through the 2020s and 2030s. The regional aircraft will be followed by the narrowbody aircraft, but only around the mid- to late-2040s. The midsize aircraft would then only follow in the mid-2050s. As the deployment of the hydrogen aircraft will be much slower and their market penetration will be much lower compared to the first scenario, PtL will need to play a much larger role. This scenario could be considered a more realistic scenario, looking at the current aviation industry statements and ambitions [1][25]. Introducing the regional aircraft first also reduces the risk for aircraft manufacturers, as it will require a lower investment in new technology. The downside is naturally that the emission reduction will be much lower, as the regional market only accounted for 7% of aviation's total CO_2 emissions (2019) [23]. In Figure 1.9 the effect of both scenarios on the fuel mix is presented and the market penetration in 2070 is shown. Additionally, the subsequent effect on CO_2 emissions is shown in Figure 1.10. In both scenarios the longest flights (>10,000 km) would be powered by SAF as this is more cost-efficient [4].

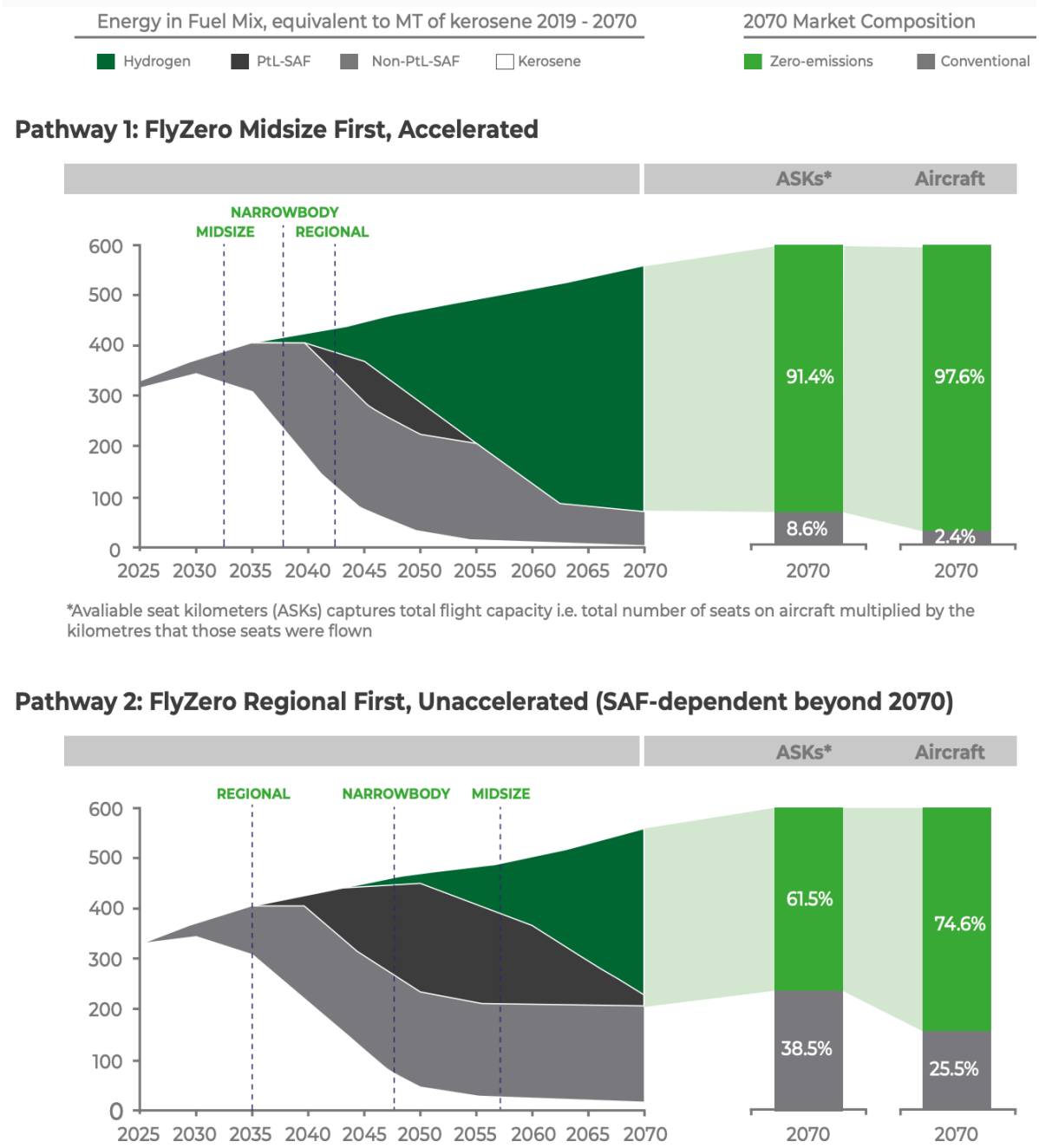

Figure 1.9: Predicted fuel mix between 2025 and 2070 for both FlyZero scenarios and the respective market penetration in 2070 [22].

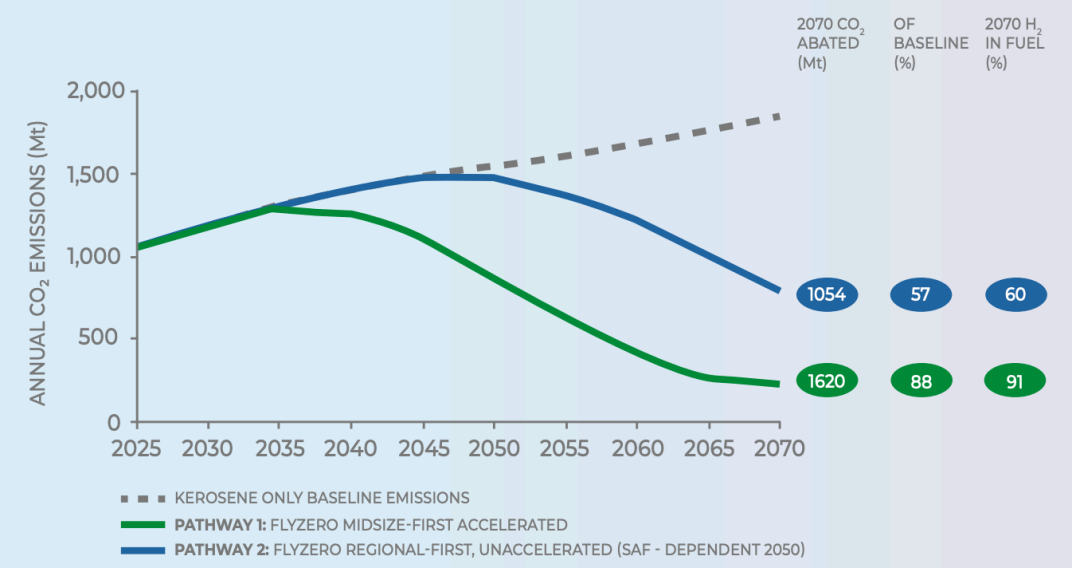

Figure 1.10: Annual CO_2 emissions for both FlyZero scenarios, compared with a kerosene only baseline scenario [23].

Clean Skies for Tomorrow (CST) [4] also defines two scenarios: an 'efficient decarbonisation' scenario, where hydrogen is deployed where it is most cost-efficient, and a 'maximum decarbonisation' scenario. For the efficient decarbonisation scenario, the cost to reduce a ton of CO_2-equivalent emission (abatement cost) using hydrogen is compared to SAFs for each range segment (commuter, regional, short-range, medium-range and long-range). As hydrogen requires a different aircraft redesign for each range segment, the abatement costs differ per segment. As SAF does not require an aircraft redesign, the abatement cost only depends on how much climate reduction can be achieved per segment. It is found that up to medium-range (and potentially including), the abatement cost for hydrogen are lower than for SAF. So in the efficient decarbonization scenario, aircraft up to, and partially including, medium-range will be replaced by hydrogen aircraft in the 2030s. The assumption is that, after an initial ramp-up, all new aircraft in the commuter, regional and short-range segments will be hydrogen powered, and 50% of new aircraft in the medium-range segment. By 2050, 40% of all aircraft would then be powered by liquid hydrogen while the remainder would be powered by SAF.
In the maximum decarbonization scenario, all aircraft with a range of up to 10,000 km would be replaced by hydrogen aircraft in the 2030s. In 2050, up to 60% of all aircraft would be powered by liquid hydrogen and the rest by SAF.
When comparing these scenarios with the FlyZero scenarios, it is clear that both CST scenarios are much more optimistic with regards to the speed at which hydrogen aviation will be rolled out. There are two likely explanations for this. Since the CST scenarios compare the abatement costs of hydrogen and SAF to determine which segments will use each fuel, an assumption is made that each aircraft will switch to either of these fuels in quick fashin. However, it does not consider the rate at which the airliners will move away from kerosene, which could be at a relatively slow pace as is assumed in the second scenario for FlyZero. The second reason is that the two CST scenarios have been specifically developed to analyse the required infrastructure in the decades up to 2050. Expected future growth and market projections have not been taken into account.
It is important to note that the general consensus is that hydrogen is not a viable option for aircraft with a range of over 10,000 km, due to the nonlinear increase in required airframe and hydrogen tank weight. For these aircraft it is more feasible and more cost efficient to power them by SAF [4].

When assessing the impact of CORSIA, which is the only agreement regarding international aviation, the results do not look very promising. CORSIA aims at stopping the growth of the net CO_2 emissions after 2020 by using SAF or via carbon offsets. However, this would not come close to reaching the 1.5 °C target from the Paris Agreement, or even 2.0 °C [21]. It is therefore clear that additional actions are necessary.

2 Methodology

The methodology that will be used to answer the research question will be laid out in this chapter. Figure 2.1 gives a high level overview of the methodology.

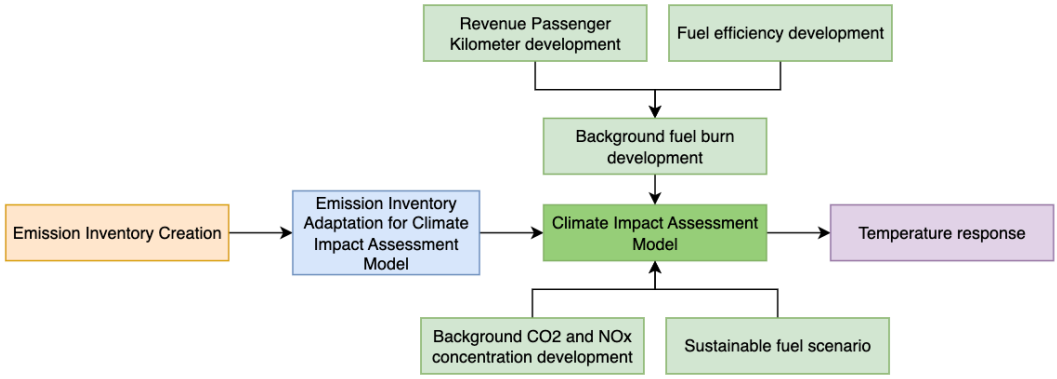

Figure 2.1: High level flowchart of the methodology. The beige, blue and green colours represent the three phases of the methodology, while the purple block is the output. The light green colour shows that these blocks serve as input to Climate Impact Assessment Model.

The first step consists of the creation of the 3D emission inventory. This emission inventory is a 3D representation of the fuel and NO_x emissions due to aviation, as well as the flown distances. For this research, a baseline emission inventory is used that was calculated as part of the Master thesis of Rik Kroon [31]. This emission inventory is based on *flightradar24* data of 2019.
As a second step, this emission inventory must be adapted and reformatted such that it is compatible with the climate impact assessment model.
Finally, the adapted 3D emission inventory is used as input to the climate impact assessment model, along with a background fuel burn development, background CO_2 and NO_x concentration developments and a sustainable fuel scenario. It is chosen to use the climate impact assessment model AirClim [20] as it has been specifically developed to analyse the impact of aircraft technology. It is one of the more modern climate impact assessment models and has been developed by V. Grewe and A. Stenke (2008).
Each aspect of the methodology will be dissected below, which is followed by a discussion of the scenarios and simulations in Section 2.4.

2.1. Emission Inventory Creation

The emission inventory is created based on flights recorded by *flightradar24* that were flown in 2019. The justification for the year 2019 is the fact that this was the last full year that was not influenced by the COVID pandemic. Due to computational limits a representative week was selected from the year 2019 for which the emission inventory was computed. The result of this was then scaled to create the emission inventory for the entire year.
For each flight in the database the flight trajectory is divided into waypoints. For each waypoint along the trajectory the point performance is calculated based on a flight performance model. This flight performance model calculates and updates the weight, altitude and airspeed of the aircraft to estimate the

fuel burn at each waypoint. This is done based on aircraft and engine performance data of EUROCONTROL [37] and the ICAO respectively [12].
Finally, from the calculated point performance at each waypoint along the flight trajectory, the emissions between the waypoints is calculated based on an emission model. This emission model uses the concept of emission index (EI) to compute the CO_2 and NO_x emissions from the fuel burn. The emission index is simply the emission quantity per unit of fuel burned. For CO_2 it was discussed in Chapter 1 that this can be calculated to be 3.15 kg per kg of fuel burned and this can be assumed to be constant throughout the flight. For NO_x the EI is dependent on the thrust setting and atmospheric conditions and is therefore not constant. The emission model uses the Boeing Fuel Flow Method 2 [11] to compute the EI of NO_x throughout the flight.
As each waypoint has a 3D location (in longitude, latitude and altitude), a 3D emission inventory is created as output. In Figure 2.2 a flowchart is presented with all the required inputs and models for the creation of the emission inventory.

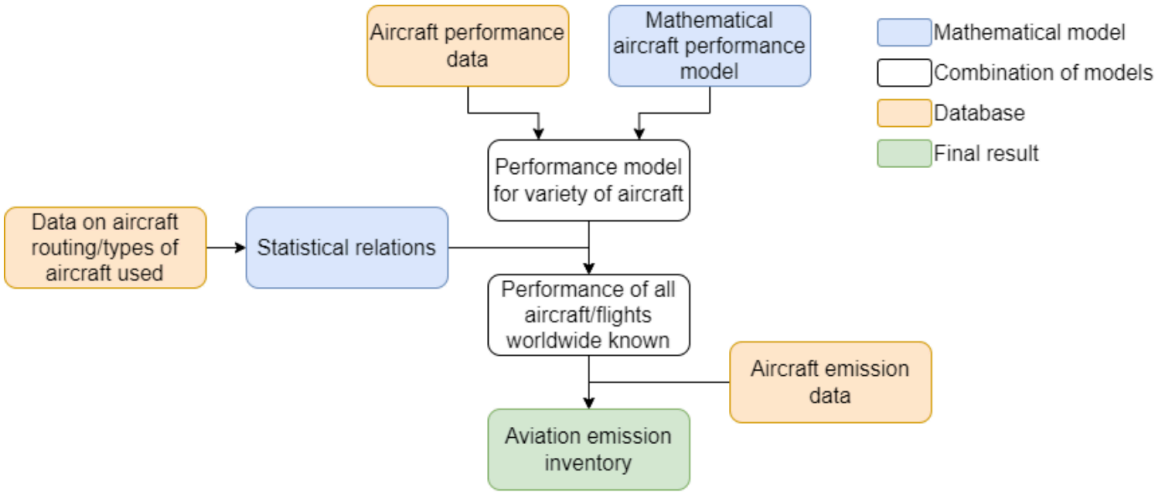

Figure 2.2: Flowchart for the creation of the emission inventory [31].

Since the emission inventory is created based on *flightradar24* data, not all flights are taken into account. Most military flights are not recorded by *flightradar24*, but if they are present in the database they are taken into account. Furthermore, the database that is used for the engine emissions data only contains jet engines. This means that all piston aircraft flights and turboprop flights are not regarded for this emission inventory. Both of these segments are relatively small compared to jet flights in terms of number of annual flights. Flights with piston aircraft only consist of around 6% of total flights [41] and these are short-range flights with only up to 10 passengers. This means that the emissions from these flights are much less than 6%. Turboprop flights are also often smaller aircraft with a shorter range compared to jet flights. According to EUROCONTROL, these flights do not make up a significant portion of aviation emissions [14]. This all leads to a total of 28,870,868 flights that are considered for the 2019 emission inventory.

This emission inventory will be compared to a very recent paper from Teoh et al. (2023), in which they have computed the 2019 emission inventory based on Automatic Dependent Surveillance–Broadcast (ADS-B) telemetry data. ADS-B is an aviation surveillance technology which an aircraft uses to determine its position via satellite navigation. With ADS-B, aircraft also periodically broadcast their position and velocity data which enables them to be tracked. This means that the emission inventory from Teoh et al. is based on actually flown trajectories.
When comparing the two emission inventories, Teoh et al. considers a significantly higher total of 40,221,182 flights. The CO_2 emissions are 4% higher and the NO_x emissions are 15% lower for Teoh et al. The total distance flown is 7% higher for Teoh et al. These numbers are important to keep in mind when comparing the results of AirClim to other research.

2.2. Emission Inventory Adaptation

To be able to use the 3D emission inventory as input to AirClim, it has to be in a specified format. An example of this is shown in Table 2.1.

Longitude [deg]	Latitude [deg]	Altitude [hPa]	Fuel [kg]	NO_x [kg]	Distance [km]	Time [yr]
-73.77	40.63	1012.77	35822.78	449.08	0.0	1.0
-73.75	40.65	842.52	6432.82	243.57	148.59	1.0
-73.73	40.66	811.39	4944.65	147.26	157.04	1.0
-73.70	40.68	781.20	5033.53	151.54	162.38	1.0
-73.67	40.69	751.93	8662.48	454.69	168.31	1.0

Table 2.1: Example of AirClim 3D emission inventory format.

Table 2.1 shows an example of how the emissions of part of a flight is stored in the 3D emission inventory. Each entry in the table represents the emissions at a waypoint along the flight trajectory. The longitude (ranging from -180 to +180 degrees), latitude (ranging from -90 to +90 degrees) and pressure altitude columns indicates the 3D location of the waypoint, while the fuel and NO_x columns represent the quantity of fuel and NO_x that is emitted between this waypoint and the previous waypoint. The distance column is then the flown distance between this waypoint and the previous waypoint. Finally, the last column indicates that these are the annual emissions at this waypoint for this flight.
In addition to these seven columns that are required as input to AirClim, five columns are also added to be able to filter the emission inventory. These five columns are the latitude and longitude location of the origin and destination airport as well as the total range of the flight. So this flight information is stored for each waypoint, such that the emission inventory can be filtered based on the geographical location of the origin and destination airport and the range of the flight.

The greatest challenge is the fact that this leads to more than 68 million waypoints, which is more than AirClim can handle as input. So a way must be found to decrease the number of rows in the emission inventory, while losing as little information as possible. As a first step, the emissions and flown distance of duplicate waypoints are combined such that only unique waypoints remain. What this means is that if the 3D location of a waypoint is identical to that of another waypoint in the emission inventory, these entries are combined and their emissions and flown distance are added together. The reason that it is possible to have duplicate waypoints comes from the fact that flight paths from separate flights may intersect, and a waypoint can be created by coincidence on this intersection during the process of dividing the flight trajectory into discrete waypoints. When there are more than 68 million waypoints, it is expected that duplicate waypoints exist.
By combining these duplicate waypoints, the number of rows in the emission inventory is reduced from more than 68 million to approximately 15 million. Note that no information is lost while doing this. The total emissions and the location of those emissions is still exactly the same.
15 million rows in the emission inventory is still too much for AirClim to handle, so a further reduction is required.
By combining duplicate waypoints, implicitly a grid with a certain resolution is created. Since waypoints will only be combined if the latitude, longitude and altitude is exactly identical, this resolution is simply the number of decimal digits at which the latitude, longitude and altitude are stored at. This means that the number of rows of the emission inventory can be further reduced by rounding the latitude, longitude and altitude. When doing this, some information about the location of the emissions will be lost. The impact that this has will need to be investigated and will be discussed further in Chapter 3. The total emissions will remain the same with this method.
By rounding the latitude and longitude to an integer and the pressure altitude to tens, only 450,899 unique waypoints remain which is sufficiently small for AirClim.

2.3. Climate Impact Assessment Model

The overall approach of AirClim is that it applies perturbations to emission input data and compares the climate impact of these perturbations with a baseline scenario. An overview of the architecture behind AirClim is shown in Figure 2.3.

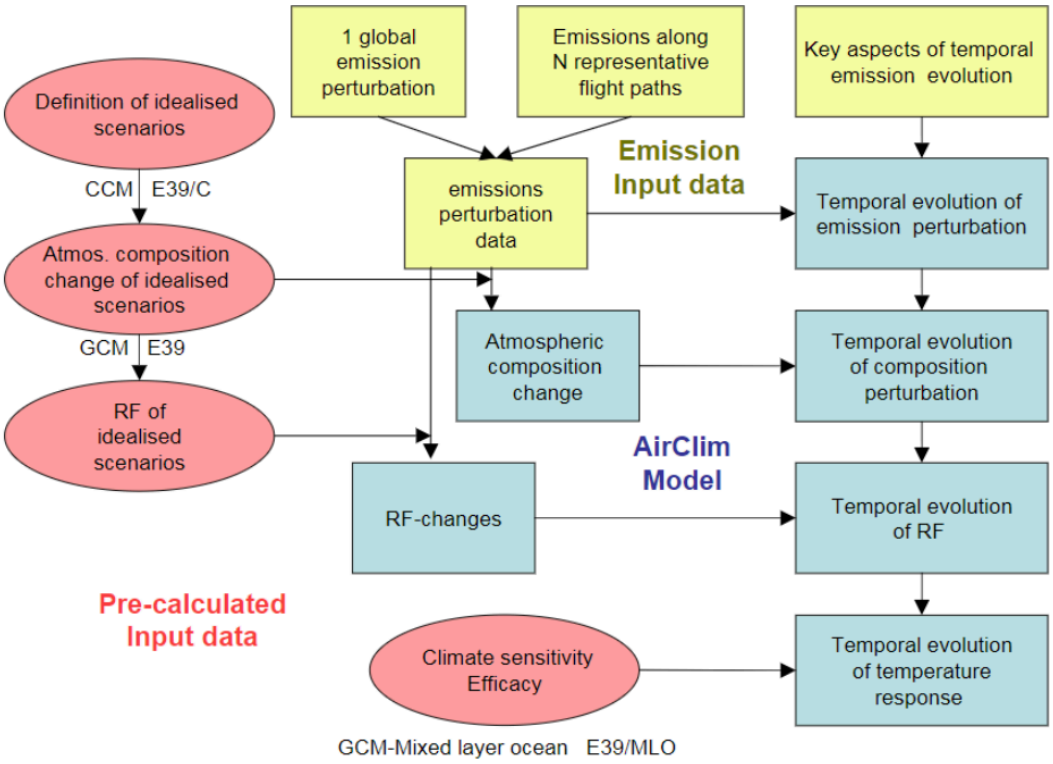

Figure 2.3: Overview of the modelling approach of AirClim [20].

The modelling approach can be deconstructed into three parts. The first (rose) part is the pre-calculated input data. In a first step, 24 emission regions with a normalised emission strength are defined. This means that each emission region has the same mass mixing ratio per unit of time. As a next step, the atmospheric composition change and the RF of the idealised scenarios is calculated with the climate chemistry model E39/C and E39 respectively. This is done for ozone, methane, water vapour and contrails. This atmospheric input data is combined with emission perturbation data (yellow boxes). The emission perturbation data consists of the 3D emission inventory and a background global emission development. By combining the emission perturbation data and the pre-calculated atmospheric input data, the atmospheric composition change and the RF-changes are calculated by AirClim (blue boxes). Another aspect of the emission input data is that of the key aspects of temporal emission evolution, which are variables like the demand growth and fuel efficiency development. This is combined with the 3D emission perturbation data to find the temporal evolution of the emission perturbation. This is in turn then first combined with the calculated atmospheric composition change of each climate agent and then with the RF-changes to obtain the temporal evolution of the RF. Finally, with the climate sensitivity efficacy of each climate agent, the temporal evolution of the RF is used to calculate the temporal evolution of the temperature response.

AirClim assumes kerosene as the fuel. This means that AirClim must be adapted when using SAF. This adaptation is required when using SAF due to the reduction in life cycle CO_2 emissions and the change in contrail properties leading to a reduction in the RF of contrails. The first aspect is discussed further down below, while the second aspect is taken into account by implementing Equation 2.1 [3].

$$\Delta RF^{\text{contr}} = \frac{\arctan\left(1.9 \triangle pn^{0.74}\right)}{\arctan(1.9)} \tag{2.1}$$

ΔRF^{contr} is the relative change (between 0 and 1) in RF for contrails when using SAF. This is a function of the relative change in particle number emissions ($\triangle pn$), which is also a dimensionless value between 0 and 1. The reduction in soot particles when using SAF is assumed to be linear, with measurements indicating that a fuel blend consisting of 50% kerosene and 50% SAF reduces the number of soot particles by 50% [36].

Besides the emission inventory, AirClim requires input regarding the temporal emission evolution. This is the background fuel burn development. The background fuel burn value is normalised in 2019 to coincide with the total emission inventory fuel burn. The emission inventory is than scaled with this background fuel burn development. How the future aviation fuel burn will develop, is driven by the future demand for aviation and the fuel efficiency gains that will be made. The background fuel burn development that will be used for all scenarios and simulations is that of the BAU (Business-as-usual) scenario from V. Grewe et al. (2021) [21]. This BAU scenario assumes that there will be further fuel efficiency gains, as has historically been the case. The same future development of the revenue passenger kilometer (RPK) and flown kilometers is used for this research as is presented in that paper. RPK is a multiplication of the number of revenue-paying passengers times the flown kilometers. This is an indication for the demand for air travel. The simulations from Grewe et al. only run until 2100, so these trends have been further extrapolated up until 2125. The RPK forecast takes the worldwide saturation effects of economic growth into account, and this has also been considered when extrapolating until 2125. This means that the RPK increases annually by 1.2% from 2025 until 2050, by 1.0% until 2075, by 0.8% until 2100 and by 0.6% until 2125. By combining the future developments in terms of fuel efficiency, RPK and flown kilometers, the future development in aviation fuel burn is found. This will then be used to scale the 2019 emission inventory.

AirClim also requires global background CO_2 and CH_4 concentrations as input. These come from the Sixth Assessment Report (2021) [6] of the Intergovernmental Panel on Climate Change (IPCC) where Shared Socioeconomic Pathways (SSPs) were introduced. These pathways describe socio-economic storylines and are accompanied by projections of concentrations for the most important climate agents. Each pathway is named by one of five storyline scenarios and their respective expected level of RF in the year 2100. For example SSP1-2.6 belongs to socio-economic scenario 1 and its estimated RF in 2100 is 2.6 Wm^{-2}.
Below is a brief description of each storyline.

- **SSP1**: This scenario is based on a world were sustainability and human well-being are more important than economic growth. Inequality is reduced across and within countries. Consumption is more focused towards being low resource and energy intensive.
- **SSP2**: This scenario is based on a world that more or less remains on a similar path as historical patterns suggest. Inequality across and within countries remains similar, or only improves slowly. Global and national institutions work towards sustainable goals but only make slow progress.
- **SSP3**: In this scenario, countries are mostly focused on their own competitiveness and security. Policies are mostly made concerning regional issues. Inequality persists or worsen over time and consumption is material-intensive.
- **SSP4**: This scenario is characterised by inequality, where an internationally-connected society contributes to capital intensive and high tech sectors of the global economy and a fragmented poorer part of the population works in labor intensive sectors. Social unrest is increasingly common and policies are diversified (both fossil fuels and green policies) but mainly focused on the middle and high income population.
- **SSP5**: In this scenario investments in fossil fuel will remain high and economic growth will be high as a result as well. For environmental problems such as air pollution and global warming, faith is put in technological advancements such as geo-engineering.

SSP2-4.5 will be used for the global background CO_2 and NO_x concentrations as this is considered a realistic middle ground scenario.
The effect of different IPCC SSPs on the temperature change will be investigated. Besides the baseline SSP2-4.5, it has been decided to investigate the effect of SSP1-2.6 and SSP3-7.0 as these are significantly different scenarios, while also being considered the more likely scenarios.
The GHG emissions for these scenarios can be summarised as follows:

- **SSP1-2.6**: Low GHG emissions where global CO_2 emissions will be net zero around 2075.
- **SSP2-4.5**: Intermediate GHG emissions where global CO_2 emissions will stay around the current level until 2050, after which it will steadily fall but have not yet reached net zero by 2100.
- **SSP3-7.0**: High GHG emissions where the global CO_2 emissions will double by 2100.

2.4. Scenarios and simulations

For the scope of this research, the simulated scenarios will be limited to only the use of SAF and not liquid hydrogen. Two different SAF scenarios will be compared to the baseline kerosene scenario. The first of these is based on the ReFuel EU legislation for SAF usage and is shown in Table 2.2.

Year	SAF blend	SAF CO_2 reduction (for 100% SAF)	Net CO_2 emissions w.r.t. kerosene
2025	2%	65%	99%
2030	6%	65%	96%
2035	20%	65%	87%
2040	34%	70%	76%
2045	42%	70%	71%
2050	70%	75%	48%
2060	90%	80%	28%
2070	99%	80%	21%
2080	99%	80%	21%
2090	99%	80%	21%
2100	99%	80%	21%
2125	99%	80%	21%

Table 2.2: ReFuel EU SAF legislation based scenario.

For the SAF blending percentage, the numbers up until 2050 are directly from the ReFuel EU legislation. From 2050 onward, the numbers have been extrapolated further with the assumptions that the SAF blending growth rate will slow down when approaching 100%. A 100% SAF usage is not reached, as it is assumed that not all remote airports and aircraft will have SAF accessibility. Remember that it is assumed that the reduction in soot particles (non-volatile Particulate Matter, i.e. nvPM) scales linearly with the SAF blend.
The 65% life cycle CO_2 reduction is mandated as part of the EU-Renewable Energy Directive (RED-II). This number is assumed to increase towards 2060 to reach an 80% net CO_2 emission reduction due to the relative increased use of PtL compared to bio-SAF. As bio-SAFs will reach their capacity limits, PtL will become increasingly important in further reducing the GHG emissions of aviation. PtL has a higher potential decrease in life cycle CO_2 emissions compared to bio-SAFs, which explains this increase from 65% to 80%.
The fourth column in Table 2.2 combines the effects of the second and third column to show the total decrease in CO_2 emissions compared to a baseline 100%. This baseline 100% is simply if no SAF and only kerosene would be used.

The second SAF scenario is a more pessimistic scenario. For this scenario it is assumed that PtL does not reach a sufficient technological maturity, which means that only bio-SAFs are used for this scenario. This scenario is shown in Table 2.3.

Year	SAF blend	SAF CO_2 reduction (for 100% SAF)	Net CO_2 emissions w.r.t. kerosene
2025	2%	65%	99%
2030	6%	65%	96%
2035	20%	65%	87%
2040	34%	65%	78%
2045	42%	65%	73%
2050	70%	65%	55%
2060	75%	65%	51%
2070	72%	65%	53%
2080	68%	65%	56%
2090	65%	65%	58%
2100	62%	65%	60%
2125	55%	65%	64%

Table 2.3: SAF scenario if only bio-SAFs are used (no PtL).

CleanSkies estimates that bio-SAFs could supply as much as the forecast jet fuel demand in 2030 if the production of bio-SAFs and their respective availability of feedstocks is optimised [35]. The result of this is that up until 2050 the SAF blend percentages are the same as for the ReFuel EU scenario. This is the case as the total used volume of SAFs in the ReFuel EU scenario will only exceed the 2030 demand after 2050. From 2060 onward, the difference between the two scenarios becomes apparent. As the total fuel demand will increase, the bio-SAF capacity will remain the same, leading to a continuous decrease in bio-SAF blending percentage after 2060. It must be noted that the total bio-SAF usage is higher for this second scenario compared to the ReFuel EU scenario, since before 2050 part of the SAF for the ReFuel EU scenario comes from PtL. The explanation for the higher bio-SAF usage in the second scenario can be found in the fact that more effort and focus will be diverted to bio-SAF when PtL does not reach the required technological maturity.
Another effect of the loss of PtL can be seen in the SAF lifecyle CO_2 reduction, which remains at 65%. The total effect that the loss of PtL has becomes most apparent when comparing the total CO_2 emission reduction of both scenarios. Where for the ReFuel EU scenario this is significantly reduced to only 21%, the loss of PtL means that this is only reduced to 51% and even increases again to 64% in 2125.

2.4.1. Monte Carlo simulation

There are large uncertainties when considering the climate impact of aviation. This is also apparent from the results of Lee et al. [33] as was shown in Figure 1.4 due to the wide range of the confidence intervals. To investigate the effect of these large uncertainties, a Monte Carlo simulation will be done. Table 2.4 shows all uncertainty parameters that will be considered and their respective range from which the value of the parameter will be drawn for each run.

Uncertainty parameter	Minimum	Maximum
Tropospheric residence time	-20%	+20%
Stratospheric residence time	-40%	+40%
Fuel burn	-20%	+20%
NO_x emission	-30%	+30%
Flown distance	-20%	+20%
CO_2 RF strength	-5%	+5%
H_2O RF strength	-50%	+50%
CH_4 RF strength	-10%	+10%
O_3 RF strength	-50%	+50%
PMO RF strength	-50%	+50%
Contrail RF strength	-50%	+50%
CO_2 climate sensitivity	-5%	+5%
H_2O climate sensitivity	-30%	+30%
CH_4 climate sensitivity	-10%	+10%
O_3 climate sensitivity	-30%	+30%
PMO climate sensitivity	-30%	+30%
Contrail climate sensitivity	-30%	+30%

Table 2.4: Uncertainty parameters with their range from which a value will be drawn for each run of the Monte Carlo simulation.

Each parameter will be drawn from a uniform distribution within the shown range. The reason a uniform distribution is chosen comes from the fact that the purpose of the Monte Carlo simulation is to investigate the spread of potential outcomes as a result of the uncertainties, so with a simple uniform distribution the spread in outcomes will be larger than for a normal distribution for example. Additionally, a normal distribution comes with the added complexity that it is unbounded (i.e. it can take a value from -∞ to +∞).
The uncertainty ranges in Table 2.4 for all parameters except for the fuel burn, NO_x emission and flown distance, follow Dahlmann et al. (2016) [8]. For the other three parameters the uncertainty range is chosen based on the discrepancy of the emission inventory with other emission inventories. For example the 2018 fuel burn according to Lee et al. (2021) [33] is 21% higher. For the NO_x emissions a discrepancy of up 30% could be found compared to other emission inventories [31]. The flown distance follows the uncertainty range of the fuel burn.
The EI for NO_x remains the same throughout all years of the simulation and this EI in itself is not an uncertainty parameter for the Monte Carlo simulation. The NO_x emission uncertainty parameter scales the NO_x emissions in the emission inventory directly, which therefore means that these emissions are independently scaled from the fuel burn uncertainty parameter for each Monte Carlo run and that there is no coupling between these two.

2.4.2. Regional simulations

As there is only a limited amount of bio-SAF available, it is interesting to investigate where this can have the most impact in reducing the near surface temperature change. The reason that a variable impact is expected when changing the emission location of SAF has to do with the change in properties of contrails when using SAF. As discussed previously, SAF reduces the RF of contrails. The climate impact of a contrail is very much dependent on the time and location at which it is formed. Therefore, it is expected that the climate impact of contrails is dependent on the SAF emission location and that there is regional effect when considering where to deploy the limited SAF. In other words, 1 kg of SAF can have a different climate impact depending on which flight it is being used for. This is solely due to contrails as the life cycle CO_2 reduction is independent of the emission location.

To investigate this hypothesis, the global emission inventory is divided into seven regions. All emissions from a flight with their origin airport in a region are counted towards that region, regardless of the location

of their destination airport. The reasoning for this is that refueling is most often done at the origin airport where the SAF would be added. This is relevant as the goal of this investigation is to identify in which region 1 kg of SAF would have the greatest impact in reducing the near surface temperature change. It is then beneficial to produce the most amount of SAF in this region and transport the most amount of SAF to this region.
The seven regions are divided in such a way that each region has approximately the same amount of flown kilometers. This is to ensure that this variable does not confound the results, as the number of flown kilometers is the primary driver behind the formation of contrails.
For each region, a simulation will be done where the baseline kerosene scenario will be compared with the ReFuel EU scenario. Finally, a metric must be defined that connects the difference in temperature for both simulations with the total fuel used for that region. This metric is shown in Equation 2.2.

$$\text{SAF impact} = \frac{T_{2125}^{kerosene} - T_{2125}^{SAF}}{\text{Total Fuel}} \tag{2.2}$$

Here $T_{2125}^{kerosene}$ is the temperature increase for the baseline kerosene scenario in the year 2125, while T_{2125}^{SAF} is the temperature increase for the SAF scenario in 2125. The numerator then represents the difference in near surface temperature in 2125 between both scenarios. The denominator is simply the total fuel used for that region in the year 2125. By dividing by the total fuel, the metric is normalised for each region and represents the avoided temperature increase per kg of SAF when comparing the ReFuel EU scenario with the baseline kerosene scenario. The unit of the metric is then simply Kkg^{-1}.

Two different sets of simulations will be done for this regional analysis. One where all the regions have the same growth rate, namely the BAU growth rate that is also used for all other simulations. For the other set of simulations, each region will have its own growth rate based on an estimation by the International Air Transport Association (IATA) [18]. It will be interesting to see if and how the individual growth rates affect the SAF impact metric results (Equation 2.2). The regional growth rates that will be used are shown in Table 2.5.

Region	**Annual RPK growth rate 2025-2040 [18]**
Africa and the Middle East (-60-46°N, -18-55°E)	3.4%
Australia and South-East Asia (-60-25°N, 55-180°E)	4.6%
China (25-56°N, 55-140°E)	4.6%
Eastern North America (34-80°N, 23-88°W)	2.2%
Europe (46-80°N, -25-14°E)	2.1%
South and Middle America (-60-33°N, 20-125°W)	2.9%
Western North America (34-80°N, 88-150°W)	2.2%

Table 2.5: Respective growth rates of each region.

Similarly as for the BAU scenario, each of the RPK growth rates will decline to 0.6% in 2125. For each region, the RPK development is combined with the flown kilometers and the fuel efficiency to get the future fuel burn development. This is then used to scale the emission inventory of each respective region.

3
Results & Discussion

All the simulation results will be presented in this chapter. In Section 3.1 the global simulation results will be discussed starting with the baseline kerosene scenario, followed by the ReFuel EU SAF scenario, the no PtL SAF scenario and the effect of the IPCC SSP background emission scenarios. This section is concluded with the results from the Monte Carlo simulation. The results of the regional analysis will be presented in Section 3.2.

3.1. Global results

3.1.1. Baseline kerosene scenario

In Figure 3.1, the temperature change from 1940 until 2125 due to the baseline kerosene scenario is shown.

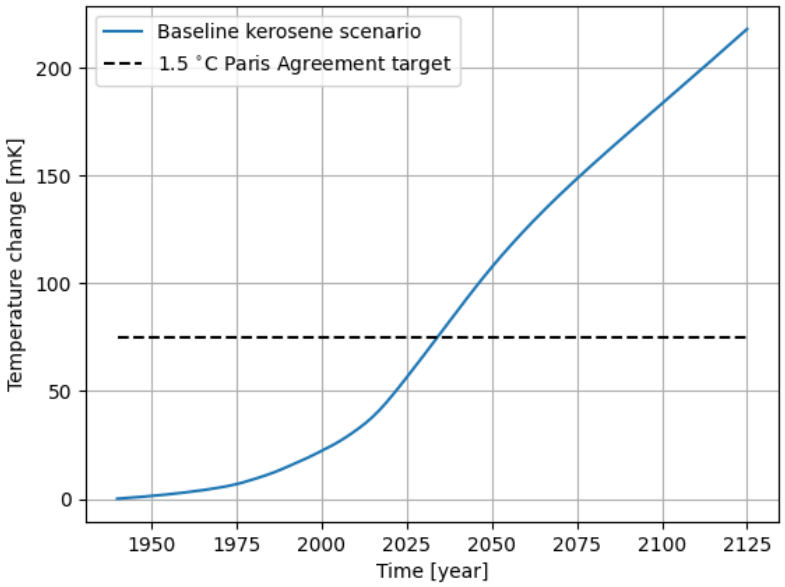

Figure 3.1: Temperature change evolution for the baseline kerosene scenario due to global aviation.

In this baseline scenario, the temperature grows quickly over the next 20 years due to the high RPK growth in the BAU scenario, after which the temperature growth declines marginally due to the slowing down of the RPK growth as a result of the worldwide saturation effects.
For reference, the Paris Agreement to limit a global temperature rise of 1.5-2.0 degrees Celsius is corresponding with 75-100 degrees mK in Figure 3.1 (5% of 1.5-2.0). This is assuming that aviation will maintain its current relative climate impact. In this baseline kerosene scenario, which assumes that historical fuel efficiency trends will continue, the 1.5 °C threshold is already crossed before 2035, with the 2.0 °C threshold following before 2050.
Figure 3.2 compares the result of this BAU baseline kerosene scenario with the same BAU scenario from Grewe et al. (2021) [21].

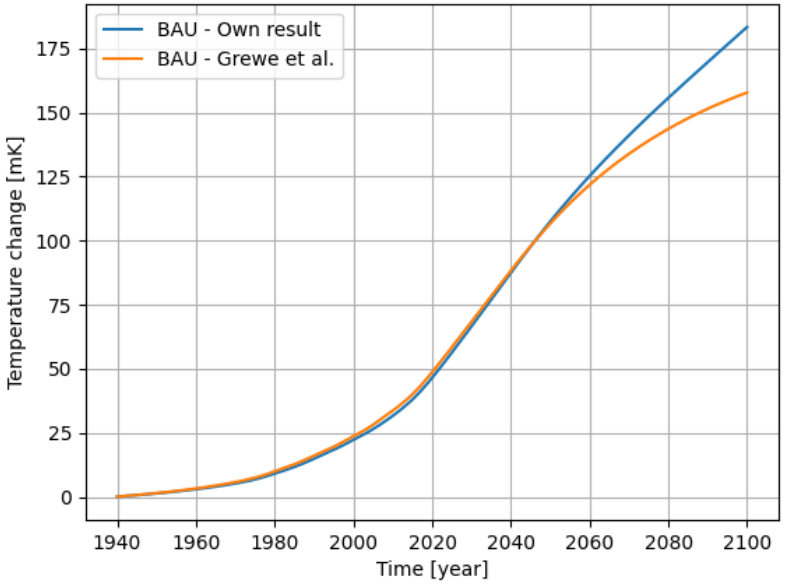

Figure 3.2: Comparison of the BAU baseline kerosene scenario with the same BAU from Grewe et al. (2021) [21].

Until 2050 the temperature evolution is almost identical, after which they slowly diverge. A large part of this divergence can be explained by the different background emission scenarios used. When using the same background emission scenario as Grewe et al., the divergence is much less significant. This can be seen in Figure 3.3.

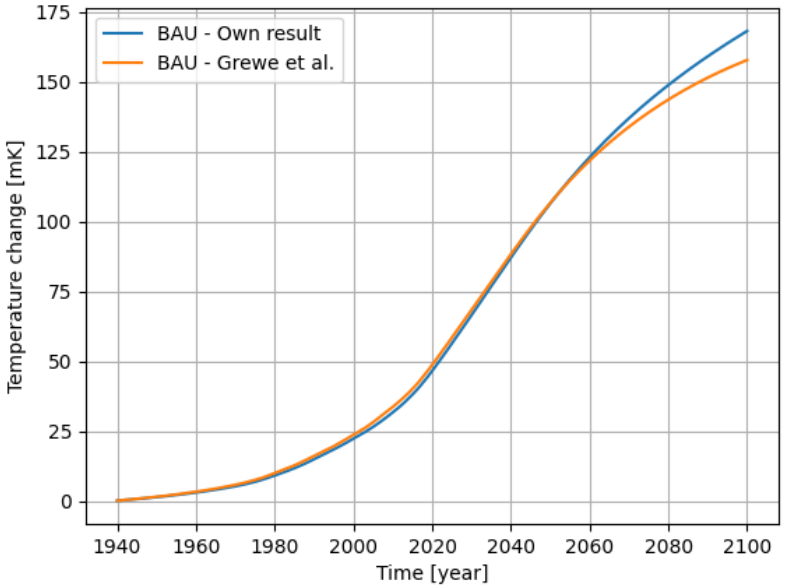

Figure 3.3: Comparison of both BAU scenarios when using the same background emission scenario [21].

The remaining divergence might be explained by the difference in emission inventory that is used for each scenario. Unfortunately the emission inventory from Grewe et al. is not available, so this will be investigated through comparisons with other emission inventories and by further dissecting the baseline kerosene scenario. Figure 3.4 dives deeper into the baseline kerosene scenario and shows

the temperature contribution of each climate agent.

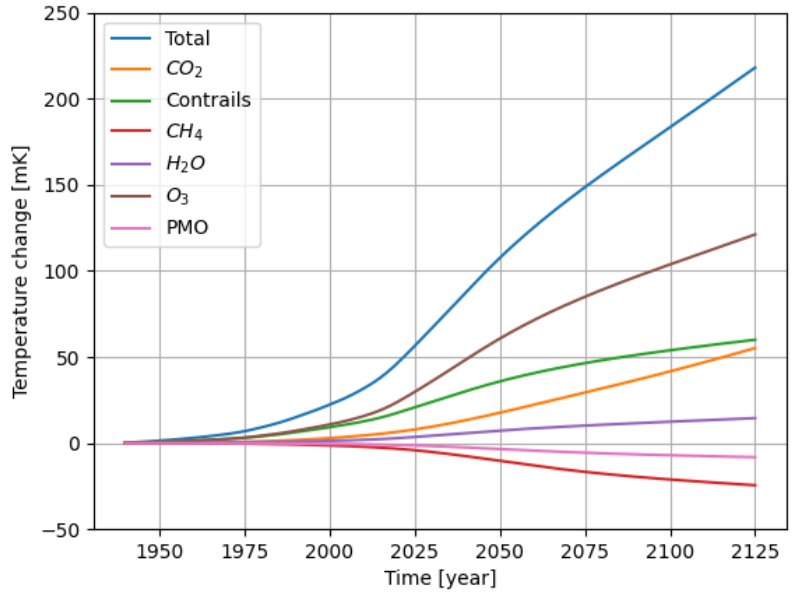

Figure 3.4: Temperature contribution of each climate agent.

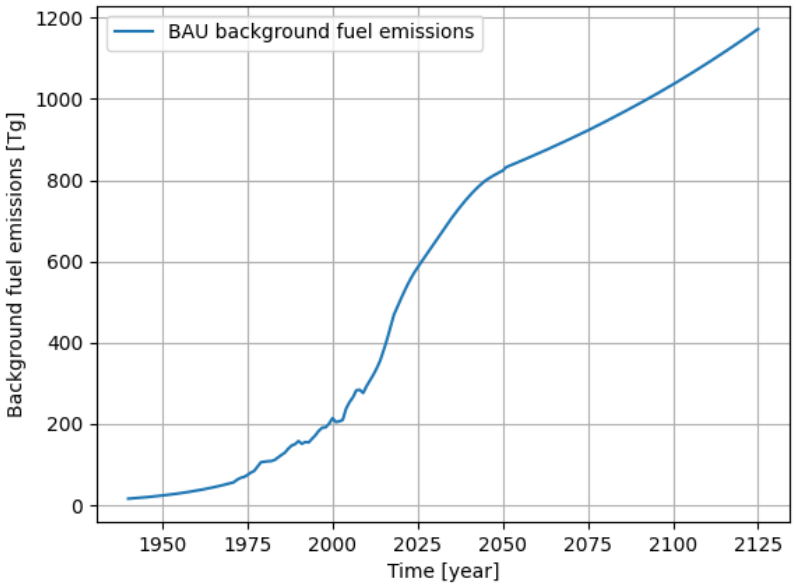

Figure 3.5: Background fuel burn for the BAU scenario. This is normalised in 2019 such that it coincides with the 2019 emission inventory fuel burn.

A couple of interesting observations can be made by looking at Figure 3.4. As expected, CH_4 and PMO have a cooling effect.
Remember that the emission inventory is scaled by the BAU scenario for which the background fuel burn is shown in Figure 3.5. When looking at Figure 3.4, the temperature contribution graph of each climate agent looks completely different. This can be explained by the difference in atmospheric lifetime

of each climate agent. For short-lived climate agents, such as contrails and ozone, the effect of an increase in emission on the temperature contribution is much quicker and more pronounced. For long-lived climate agents, such as CO_2 and CH_4, it takes much longer before an effect can be seen due to an increase in emissions. This difference between short- and long-lived climate agents is even more apparent when comparing the temperature response and the emission inventory scaling with the RF response (Figure 3.6).

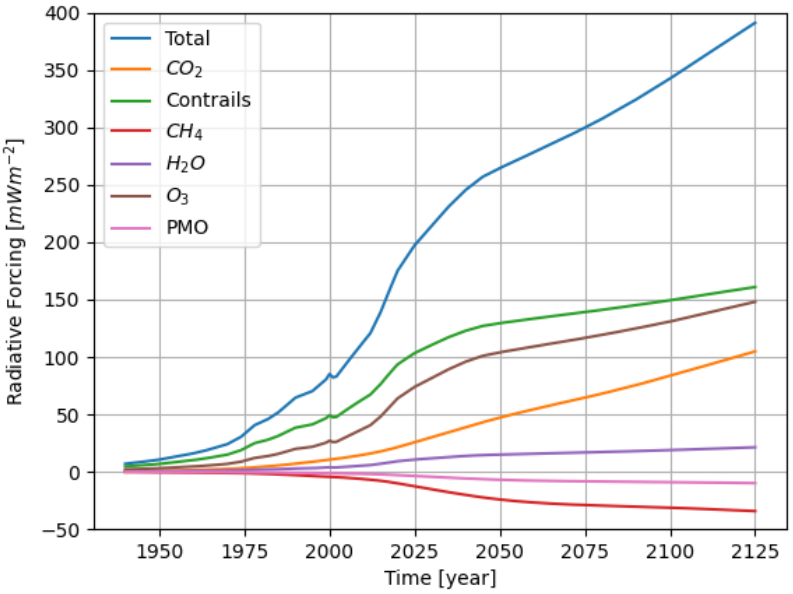

Figure 3.6: Radiative Forcing contribution of each climate agent. The small decline in 2001 and 2002 is explained by the dot.com bubble burst and the following brief financial crisis in (mostly) the developed countries.

For the short-lived climate agents, contrails and ozone, the RF response looks very similar to the background fuel burn of the BAU scenario. This is as expected, as an increase in their emission should lead to an almost instantaneous increase in RF. For CO_2 and CH_4, this increase in emission leads to a slower, more gradual increase in RF over time. These increases in RF then translate to an increase in the temperature. This explains why each graph in Figure 3.4 looks the way it does.

Coming back to the slight divergence between the BAU baseline kerosene scenario and the Grewe et al. BAU scenario that could be seen in Figure 3.3, Table 3.1 might give more insight into this. Table 3.1 shows a comparison of the relative temperature contribution in 2005 and 2100 between both BAU scenarios.

Climate agent	**2005 temperature contribution**	**2100 temperature contribution**	**2005 temp. contr. Grewe et al.**	**2100 temp. contr. Grewe et al.**
CO_2	14%	23%	25%	41%
Contrails	40%	29%	33%	22%
NO_x	40%	41%	41%	36%
H_2O	6%	7%	1%	1%

Table 3.1: Comparison of the relative temperature contribution in 2005 and 2100 between the BAU baseline kerosene scenario and the Grewe et al. (2021) BAU scenario [21].

There are two main differences when comparing the respective individual values in Table 3.1. The CO_2 contribution is significantly lower, while the H_2O contribution is much higher. These two differences can be explained by looking at the emission inventory. For the 2019 emission inventory from Rik Kroon, it is

known that the fuel burn is on the lower side when compared to other emission inventories (for example 21% lower compared to Lee et al (2021) [33] and 18% lower compared to US Energy Information Administration). For the high H_2O contribution something else is going on. By diving deeper into the methods that Rik Kroon used to create the emission inventory, it is found that the maximum altitude for each aircraft type is used as its cruise altitude when determining its flight trajectory. This means that the average cruise altitude is on the high side. As discussed in Chapter 1, the atmospheric lifetime of H_2O increases significantly with increasing altitude, which in turn increases its climate impact. This would explain the difference in H_2O contribution with respect to Grewe et al. Since the emission inventory from Grewe et al. is not available, this hypothesis is investigated via a comparison with the 2019 emission inventory from Teoh et al. (2023) [42]. Figure 3.7 shows the comparison of the probability density function of the annual fuel burn by altitude of the Rik Kroon emission inventory with the emission inventory from Teoh et al.

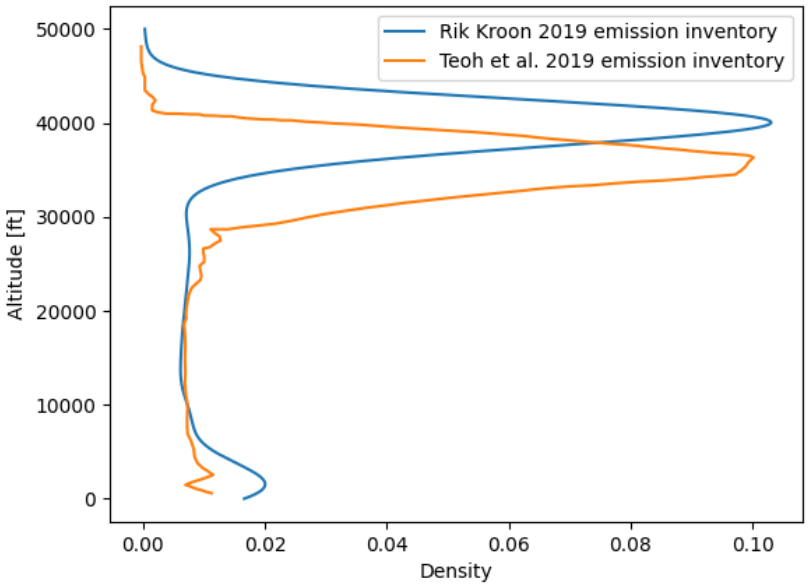

Figure 3.7: Comparison of the probability density function of the annual fuel burn by altitude between the 2019 Rik Kroon emission inventory and the 2019 Teoh et al. (2023) emission inventory [42].

Figure 3.7 shows that the Rik Kroon emission inventory is shifted towards higher altitudes. This confirms that the average cruise altitude is higher for the Rik Kroon emission inventory as the peak of the probability density function is around 40,000 feet, compared to around 36,000 for Teoh et al. This higher average cruise altitude can therefore explain the higher H_2O contribution that is observed in Table 3.1 compared to Grewe et al.

What is more relevant for the comparison in Table 3.1 is that the temperature contribution trends when going from 2005 to 2100 is similar. In both cases the relative contribution of CO_2 increases drastically, while that of contrails decreases. The reason for this has again to do with the difference in atmospheric lifetime. The temperature contribution of contrails is more correlated with its emission, as it has a very short atmospheric lifetime meaning that its RF response is almost instantaneous. As the growth in emissions slows down from 2040, as is shown in Figure 3.5, the temperature contribution growth of contrails will also slow down. Due to the very long atmospheric lifetime of CO_2 (lifetime of centuries), its temperature contribution growth does not slow down towards 2100. It actually keeps on increasing until the end of the simulation, as its temperature response to the slowed down growth of its emission is much delayed. This means that in 2100 the relative temperature contribution of CO_2 is much higher compared to 2005, and for contrails the opposite is the case. For NO_x and H_2O their relative contribution remains similar, although Grewe et al. shows a small decrease for NO_x.

Table 3.1 can also explain the divergence that is still observed in Figure 3.3. The relative temperature contribution of CO_2 is much lower in 2100 when comparing to Grewe et al., while the relative contribution of the short-term climate agents is higher. As discussed above, this higher portion of short-term climate agents means that the temperature graph will follow the emission and RF graph closer, as they are more correlated in this case. This behavior can be observed in Figure 3.3 where the blue line keeps increasing more, which is in line with the emission graph.

In Table 3.2 a final comparison is made to other literature, that of Lee et al. (2021) [33] which was also shown in Figure 1.4. Table 3.2 compares the RF of each climate agent from 1940-2018/2019.

Climate agent	**RF (mWm^{-2})**	**RF Lee et al. (mWm^{-2})**
Contrails	90.25	111.4 [33, 189]
CO_2	20.64	34.3 [31, 38]
O_3	60.75	36.0 [23, 56]
PMO	-2.75	-9.0 [-17, -6.3]
CH_4	-9.56	-17.9 [-34, -13]
H_2O	8.75	2.0 [0.8, 3.2]
Total	**168.08**	**149.1 [70, 229]**

Table 3.2: Comparison of the RF of each climate agent from 1940-2018/2019. The second column shows the RF of the BAU baseline kerosene scenario from 1940-2019, while the third column shows the RF from 1940-2018 from Lee et al. (2021) [33]. In the third column the 5%-95% confidence interval is also shown in brackets.

The reason that 2019 is chosen for the BAU baseline kerosene scenario, is due to the fact that the emission inventory is introduced in 2019. As can be seen in Table 3.2, similar results as for the comparison to Grewe et al. are obtained. The RF of CO_2 is lower due to the 21% lower fuel burn in the emission inventory. The RF of NO_x is higher both due to the higher NO_x emissions as well as the higher cruise altitude, as NO_x emissions also have a greater climate impact with increasing altitude. Another reason for the much higher climate impact of NO_x emissions is the underestimation of the impact of these emissions in previous research due to methodological short-comings in the calculation of its climate impact [19]. Most aspects of these short-comings have been addressed in the latest iteration of AirClim, and this higher NO_x RF is also in agreement with the results of Grewe et al. (2021) [21]. This explains the much higher climate impact of NO_x emissions compared to Lee et al. [33]. From the three explanations for the higher RF of NO_x, this last one has the greatest impact.
The higher H_2O RF is again explained by the higher cruise altitude. The total climate impact in terms of RF is of a similar magnitude.

3.1.2. ReFuel EU SAF scenario

Figure 3.8 shows the temperature change comparison between the baseline kerosene scenario and the ReFuel EU SAF scenario.

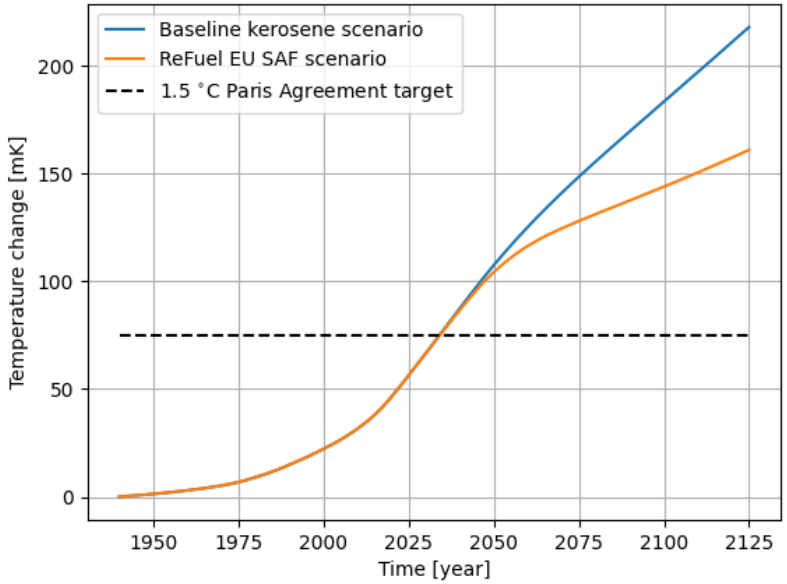

Figure 3.8: Temperature change evolution for the baseline kerosene scenario and the ReFuel EU SAF scenario.

The impact of the SAF use is very noticeable from 2050 onward, where the growth in temperature is significantly reduced. This is solely the effect of the reduced temperature contribution of CO_2 and contrails, as the other climate agents are unaffected by the use of SAF. This can be seen in Figure 3.9 and Figure 3.10, where a side by side comparison is shown between the temperature contribution of each climate agent for the ReFuel EU SAF scenario (Figure 3.9) and again the baseline kerosene scenario (Figure 3.10). The same y-axis scale is used for both figures such that the difference is clearly visible.

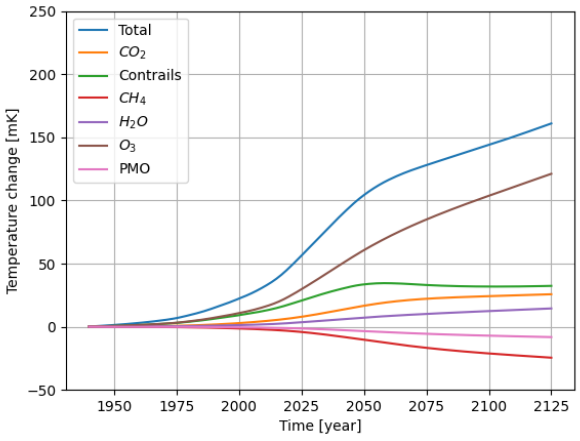

Figure 3.9: Temperature contribution of each climate agent for the ReFuel EU SAF scenario.

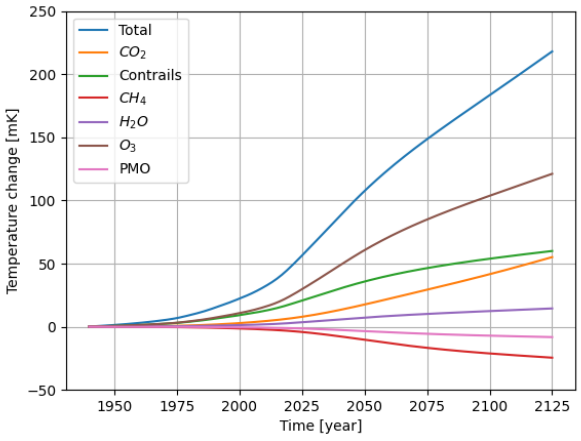

Figure 3.10: Temperature contribution of each climate agent for the baseline kerosene scenario.

As can be seen in Figure 3.9, the temperature contribution of contrails starts to decrease after 2050 when the SAF blend percentage reaches a sufficient level to compensate for the increase in the flown kilometers. The temperature contribution of CO_2 does not decrease at any point due to its delayed and leveled off response as a result of its much longer atmospheric lifetime. The reduced growth of the CO_2 temperature contribution is clearly visible when comparing to the baseline kerosene scenario.

In Figure 3.11 and Figure 3.12 the same comparison is shown for the RF contribution of each climate agent.

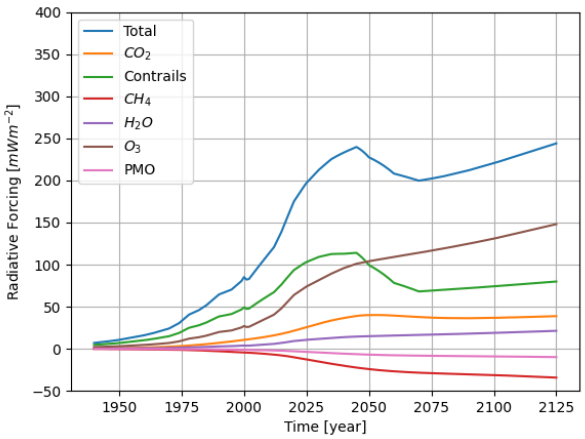

Figure 3.11: Radiative Forcing contribution of each climate agent for the ReFuel EU SAF scenario.

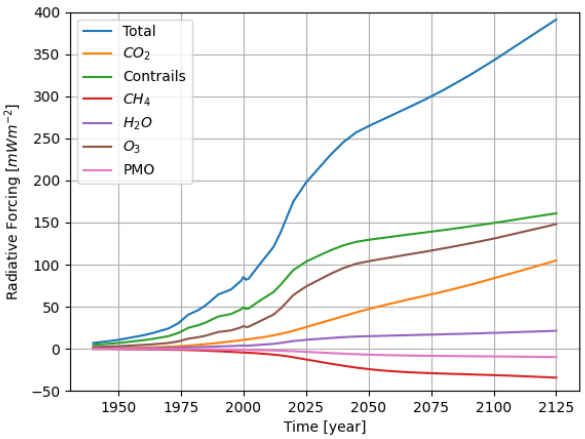

Figure 3.12: Radiative Forcing contribution of each climate agent for the baseline kerosene scenario.

In the RF comparison the difference between the two scenarios is even more noticeable. A steep decline in RF is seen for contrails just before 2050 for the ReFuel EU SAF scenario. As stated above, this is the result of the increasing SAF blend percentage. This time a reduction is also visible for the CO_2 RF, albeit a slight one. After the initial reduction for both the contrail RF as well as the CO_2 RF, the RF increases again at a steady rate. This is due to the fact that the SAF blend percentage and net reduction in life cycle CO_2 emissions is not changing anymore after 2070, when the maximum potential for SAF is reached. The emission scaling does still increase further from 2070 onward (Figure 3.5), which results in this increase in RF.

The above results show the importance of the non-CO_2 climate agents. Even with the significant use of SAF in the ReFuel EU scenario (resulting in a net 79% CO_2 reduction from 2070 onward), it exceeds the 1.5-2.0 °C Paris Agreement goal by a significant margin. Especially the unaffected NO_x emissions hurt the climate impact gains that can be achieved. This shows that efforts to reduce the NO_x emissions are of vital importance. These results also stress the potential for liquid hydrogen powered aircraft in this regard, as that can reduce the NO_x emissions by around 50-80% for gas turbine powered aircraft or 100% for fuel cell propulsion. A note here is that this effect might also be exaggerated in this research due to the higher ozone climate impact and reduced cooling of PMO and CH_4 compared to Lee et al. (2021) [33]., such that the net NO_x climate impact is much higher. However, as mentioned previously, the climate impact of NO_x emissions is probably understated in previous research due to methodological short-comings in the calculation of the climate impact of aviation's NO_x emissions [19].

Finally, the impact of reducing the number of waypoints in the emission inventory by rounding the latitude, longitude and altitude must be investigated. Remember that by doing this, only some information regarding the location of the emissions is lost and that the total emissions remain the same. The comparison between the above results (with 450,899 waypoints) and a higher resolution result (with 4,975,962 waypoints) for both the baseline kerosene scenario and the ReFuel EU SAF scenario is presented in Figure 3.13.

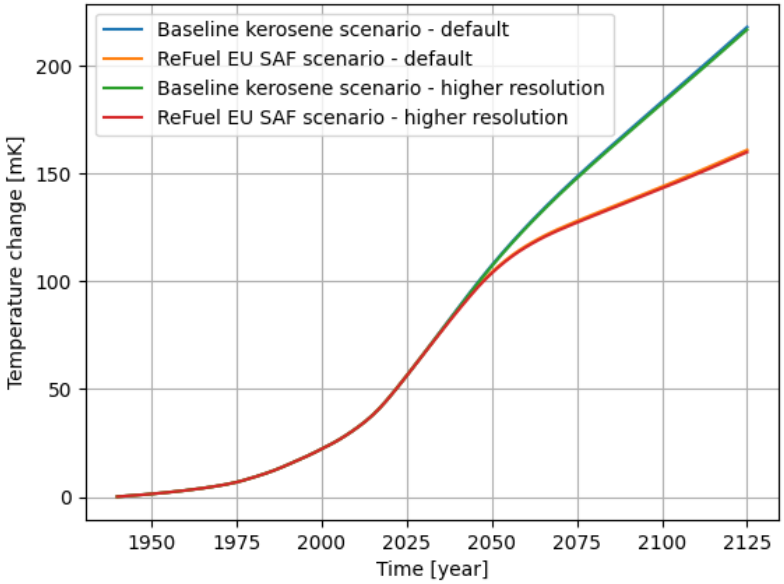

Figure 3.13: Comparison in temperature change result between a higher resolution (with 4,975,962 waypoints) and the default resolution (with 450,899 waypoints) emission inventory for both the baseline kerosene scenario and the ReFuel EU SAF scenario.

As can be seen in Figure 3.13, the high resolution result and the default resolution result are almost indistinguishable from each other. For both scenarios, the absolute difference in 2125 with the high resolution result is less than 0.62%. This shows that the method for reducing the number of waypoints in the emission inventory does not affect the results in a significant way.

3.1.3. No Power-to-Liquid SAF scenario

In Figure 3.14, the no PtL SAF scenario is also added to the temperature change evolution graph.

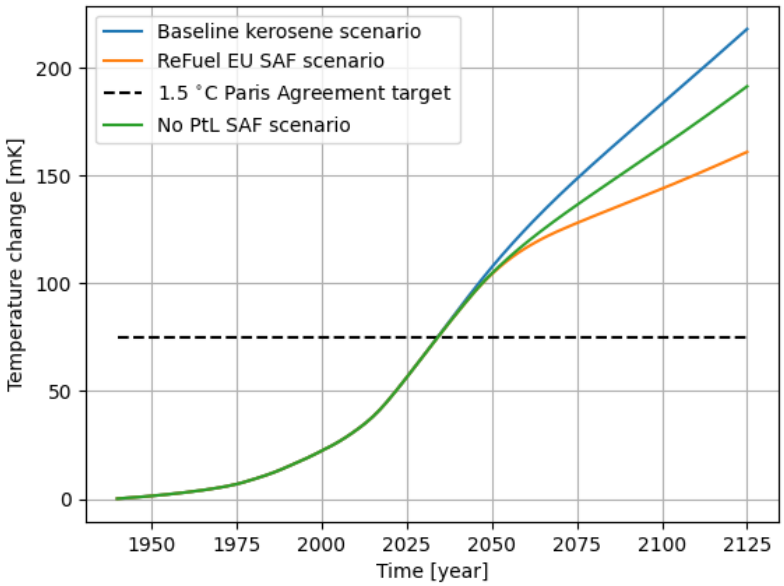

Figure 3.14: Temperature change development comparison with the addition of the no PtL SAF scenario.

The no PtL SAF scenario results in a temperature change in 2125 which falls in between the baseline kerosene and ReFuel EU SAF scenarios. When comparing the result of this scenario with that of the ReFuel EU SAF scenario, the impact of the loss of PtL as a SAF is clear. Until 2060 the difference is minimal, however from 2060 onward the impact is clear. The is as expected, as the SAF blend percentage is the same until 2050 (although the net reduction in life cycle CO_2 emissions is slightly less for the no PtL scenario). After 2050, when the maximum bio-SAF potential is reached (so without PtL), the difference becomes noticeable. This shows the importance of PtL when relying on SAF, as the ReFuel EU scenario, which uses PtL, achieves more than double the temperature reduction in 2125 compared to the baseline kerosene scenario as the no PtL scenario.

3.1.4. IPCC SSP scenario results

Figure 3.15 shows the comparison for the temperature change evolution when using the SSP1-2.6 and the SSP3-7.0 as background emission scenarios versus the default SSP2-4.5 background emission scenario.

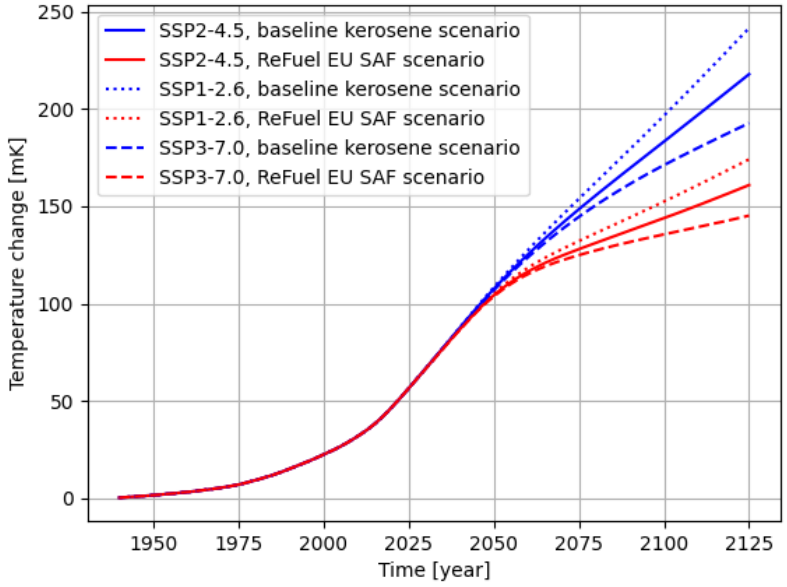

Figure 3.15: Temperature change evolution comparison for the SSP1-2.6 and the SSP3-7.0 background emission scenarios versus the default SSP2-4.5 background emission scenario.

As can be seen in Figure 3.15, the lower background emission scenario for SSP1-2.6 results in a higher temperature change contribution for aviation, both in relative as in absolute terms. This might at first glance seem counterintuitive, but it can be explained easily. Remember that in both scenarios, the absolute emissions due to aviation are the same. However when other non-aviation emissions are reduced (i.e. a lower background emission scenario), the relative impact of these aviation emissions are higher. This leads to a higher temperature change due to aviation. Furthermore, consider the effect of a pulse emission on the temperature change. Initially the temperature will increase due to this pulse emission, and with this increase in temperature the amount of outgoing radiation from earth will also increase. This will continue until a new temperature is reached at which the incoming and outgoing radiation is equal again. When the same pulse emission would now be emitted again the temperature will not rise as much as before, as the relative magnitude of this second pulse emission is lower. Now admittedly, this simplified example does not consider the non-linearities and positive and negative feedback loops in earth's climate system, but it does help understand why a lower background emission scenario results in a higher temperature change for the same aviation emissions.

Unsurprisingly, the opposite effect can be observed for SSP3-7.0. The higher background emission scenario results in a lower relative and absolute aviation climate impact. The impact that this background

emission scenario has is very significant: the absolute difference in temperature in 2125 between the SSP1-2.6 and the SSP3-7.0 is 48.91 mK for the kerosene scenario. This is not far off from the impact that the ReFuel EU SAF scenario has compared to the baseline kerosene scenario, with the default SSP2-4.5 as background emission scenario. This difference is 57.03 mK in 2125.

3.1.5. Monte Carlo simulation

The Monte Carlo simulation consists of 3000 individual runs. All drawn parameters for every run have been recorded for reproducibility purposes. Figure 3.16 and Figure 3.17 show the results of the first 100 runs for both the baseline kerosene scenario as well as the ReFuel EU SAF scenario. The default results for both of these scenarios have also been added as a reference. The same y-axis scale is again used for both figures.

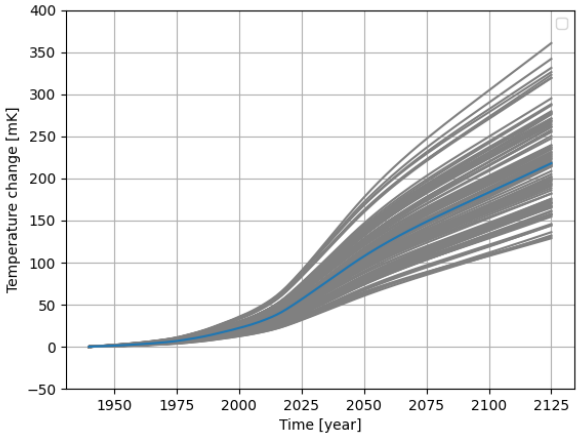

Figure 3.16: Result of the first 100 Monte Carlo simulation runs for the baseline kerosene scenario. The blue line is the default baseline kerosene scenario.

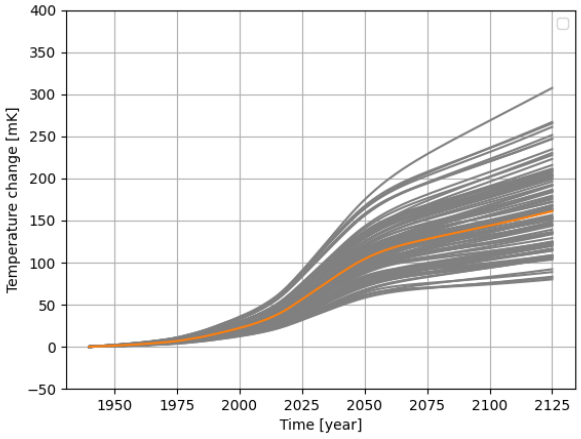

Figure 3.17: Result of the first 100 Monte Carlo simulation runs for the ReFuel EU SAF scenario. The orange line is the default ReFuel EU SAF scenario.

The first thing that comes to mind when looking at Figure 3.16 and Figure 3.17 is the large spread of outcomes of the runs. This is not unexpected as the uncertainty ranges for the parameters are rather large (up to $\pm$50%). The same can be seen from the Monte Carlo simulation of Grewe et al. (2021) [21], which uses the same uncertainty ranges. This Monte Carlo simulation uses an additional 6 uncertainty parameters, so a larger spread is expected. This result further emphasises the large uncertainties that are associated with the climate impact of aviation.

Figure 3.18 and Figure 3.19 presents the 5th and 95th percentile for the baseline kerosene and the ReFeul EU SAF scenario respectively, which again shows the large spread in results from the Monte Carlo simulation.

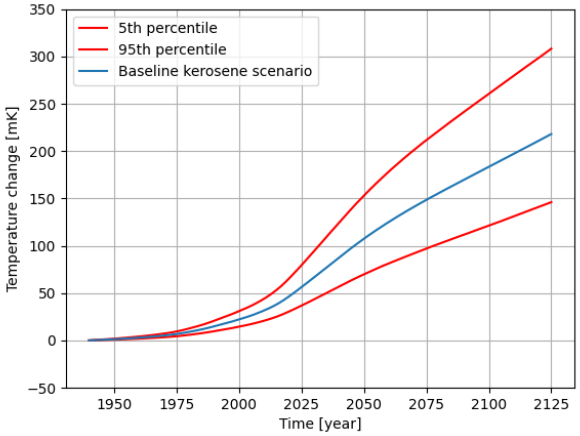

Figure 3.18: 5th and 95th percentile for the baseline kerosene scenario.

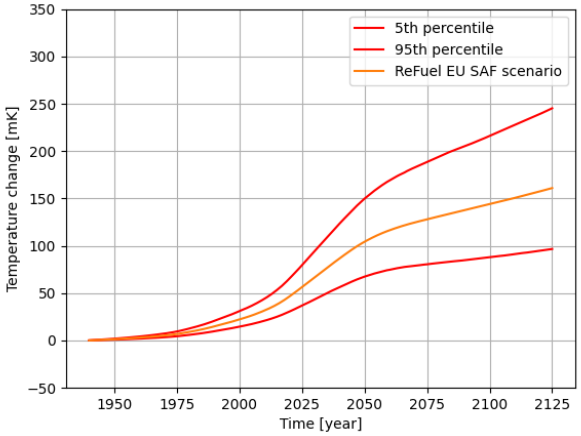

Figure 3.19: 5th and 95th percentile for the ReFuel EU SAF scenario.

Another observation that can be made from Figure 3.18 and Figure 3.19 is the fact that the absolute difference between the 95th percentile and the default scenario is higher than the absolute difference with the 5th percentile for both the baseline kerosene scenario as well as the ReFuel EU SAF scenario. This means that the outcomes of the Monte Carlo simulation are slightly skewed towards the higher temperature changes when compared to the respective default scenario. This shows the non-linearities in the climate model as the uncertainty ranges for all parameters from the Monte Carlo simulation are symmetrical.

Finally, when comparing the results of the Monte Carlo simulation with the 1.5-2.0 °C Paris Agreement goal, only 6.9% (206 out of 3000 runs) of the ReFuel EU SAF scenario results stayed below the 100 mK threshold (corresponding to 5% of 2.0 °C) in 2125. Only 0.3% (9 out of 3000 runs) stayed below the 75 mK threshold (corresponding to 5% of 1.5 °C). For the baseline kerosene scenario not a single run stayed below the 100 mK threshold in 2125.
These results show that for aviation to accomplish its relative contribution to limit global warming with 1.5-2.0 °C, an initial overshoot towards this goal is almost inevitable. This is also what previous research has concluded.

3.2. Regional results

For the regional analysis the aim was to determine the region where the use of 1 kg of SAF would have the highest reduction in temperature compared to the baseline kerosene scenario. This is done by specifically looking at the contrail temperature contribution as this is dependent on the emission location. Figure 3.20 and Figure 3.21 show the results of the contrail temperature contribution for the baseline kerosene scenario and the ReFuel EU SAF scenario for all regions.

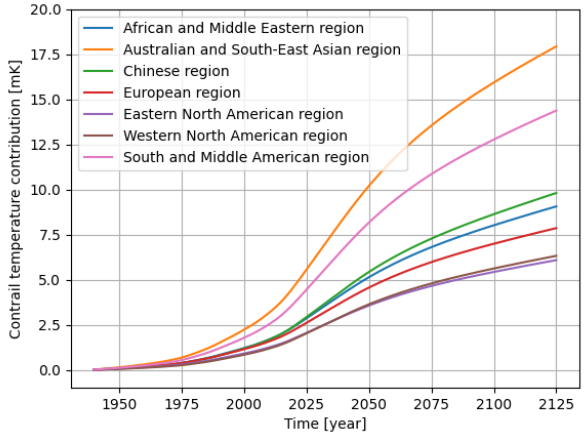

Figure 3.20: Contrail temperature contribution for all seven regions for the baseline kerosene scenario.

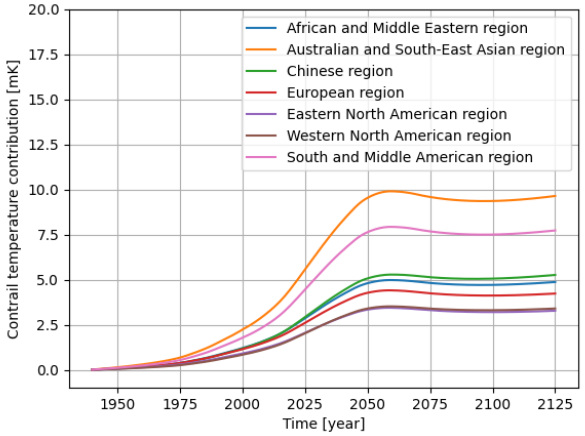

Figure 3.21: Contrail temperature contribution for all seven regions for the ReFuel EU SAF scenario.

From the above figures it is apparent that there are considerable differences between the regions, despite the fact that each region has approximately the same number of flown kilometers. The Australian and South-East Asian region has the highest contrail temperature contribution, followed by the South and Middle American region. This can be explained with the help of Figure 1.2. This figure shows that the highest probability for a persistent contrail to form is around the cruise altitude (especially considering the higher cruise altitude of the emission inventory) at the equator, and slightly lower around the poles. This means that regions which have many flights at cruise altitude around the equator are expected to have a higher contrail temperature contribution.
When looking at Australia for example, almost all international flights from Australia fly at cruise altitude around the equator. This includes flights from Australia to Japan, China, South-East Asia, Middle East and even North America. Similarly, South-East Asia itself lies close to the equator and therefore has many flights that are flying at cruise altitude around the equator, such as to Australia and within South-East Asia itself. It is therefore no surprise that this region has the highest contrail temperature contribution. The same goes for the South and Middle American region. Many of the flights from this region go to North America and Europe where they fly around the equator at cruise altitude.
The reason that Europe and both North American regions have a much lower contrail temperature contribution comes from the fact that many of the flights from these regions fly to destinations within their region (and are therefore not close to the equator), or fly from Europe to North America or vice versa. Therefore this last selection of flights does also not fly close to the equator.
As expected, the absolute difference between the baseline kerosene scenario and the ReFuel EU SAF scenario is higher for regions with a higher contrail temperature contribution.

By comparing the probability density function of the flown distance by latitude between all regions, the above explanations can be substantiated. Since the probability density function of the flown distance by altitude for each region looks identical to that of the global emission inventory (which is presented in Figure 3.7), it is sufficient to only look at the latitude distribution for this. Figure 3.22 until Figure 3.28 show these latitude distributions per region.

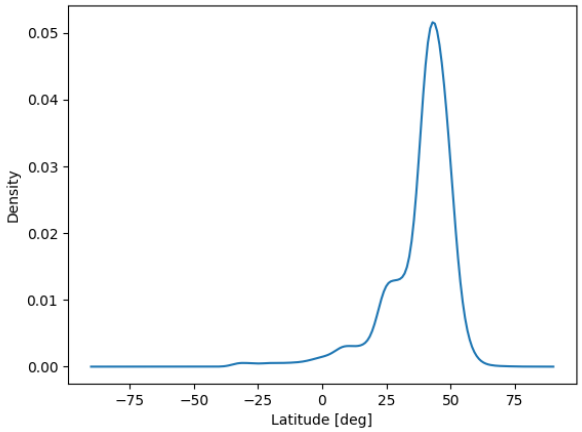

Figure 3.22: Probability density function of the flown distance by latitude for the African and Middle Eastern region.

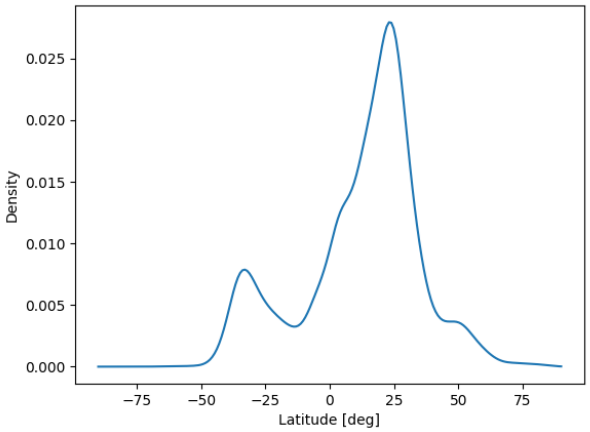

Figure 3.23: Probability density function of the flown distance by latitude for the Australian and South-East Asian region.

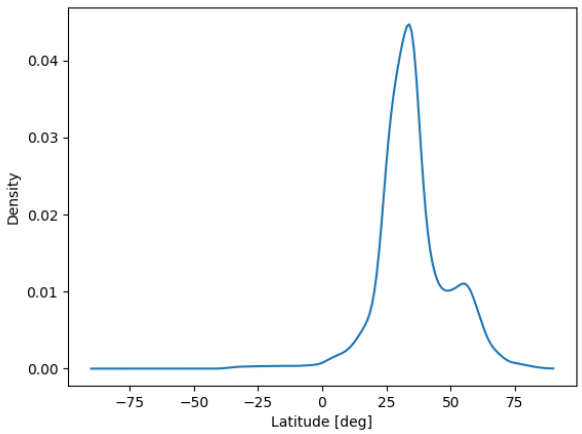

Figure 3.24: Probability density function of the flown distance by latitude for the Chinese region.

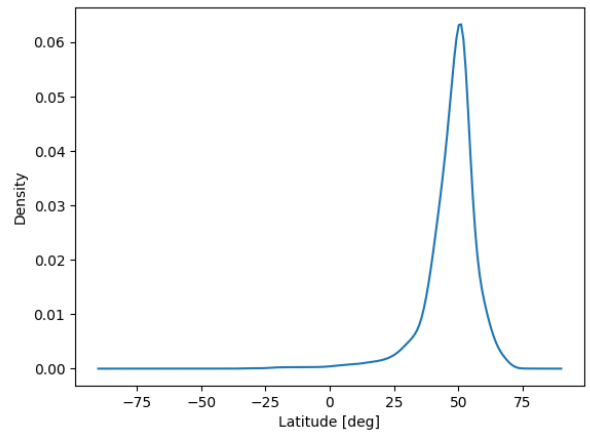

Figure 3.25: Probability density function of the flown distance by latitude for the European region.

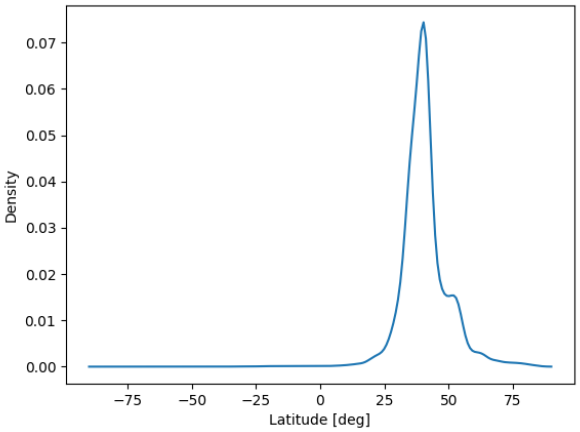

Figure 3.26: Probability density function of the flown distance by latitude for the Eastern North American region.

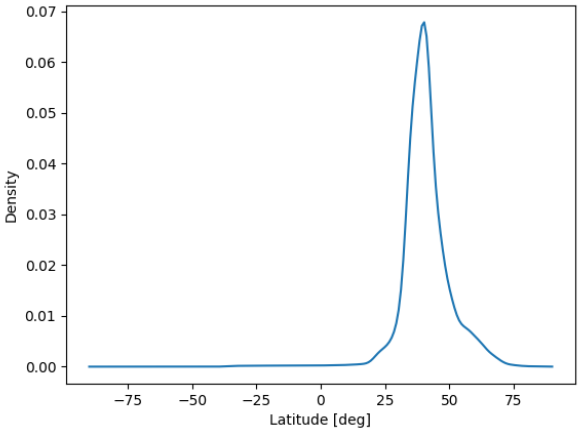

Figure 3.27: Probability density function of the flown distance by latitude for the Western North American region.

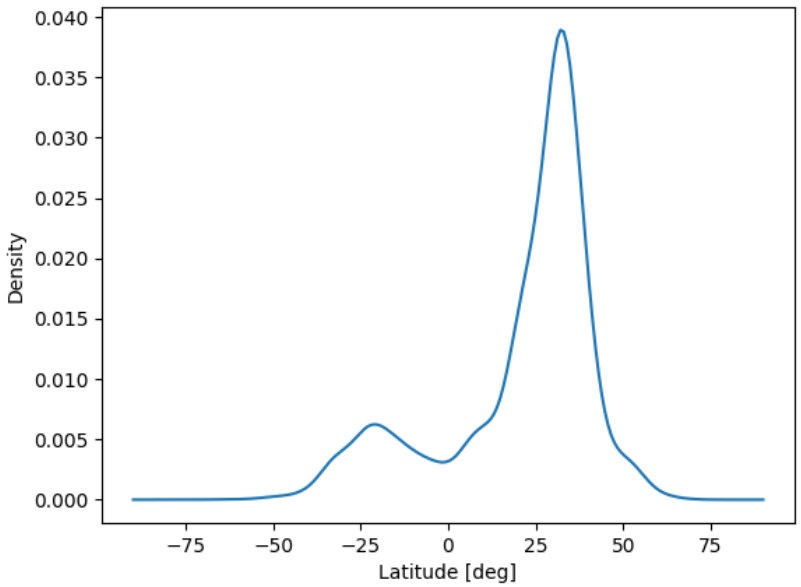

Figure 3.28: Probability density function of the flown distance by latitude for the South and Middle American region.

From Figure 3.22 through Figure 3.28 it is apparent why the Australian and South-East Asian region has the highest absolute contrail temperature contribution. Figure 3.23 shows that the latitude region where the most kilometers are flown, is the closest to the equator for the Australian and South-East Asian region compared to all other regions. As mentioned previously, regions with many flown cruise kilometers close to the equator will have a high contrail temperature contribution as the probability that a persistent contrail will form is high here. The same can be seen to a lesser extend for the South and Middle American region (Figure 3.28). This explains why this region has the second highest contrail temperature contribution. These two regions are also the only two regions for which a local maximum at negative latitudes can be seen in the graph. This indicates that these two regions have more flights at cruise altitude that fly near and across the equator.

These graphs also show why the Eastern and Western North American regions and the European region have a much lower contrail temperature contribution. For these three regions the peak of the probability density function is located at much higher latitudes further away from the equator, where the

probability of contrail formation is lower.
Table 3.3 shows the result per region on a per kg SAF basis, as defined by the metric discussed in Section 2.4.2 (Equation 2.2).

Region	SAF impact - BAU (10^{-11} mKkg^{-1})	SAF impact - growth rate (10^{-11} mKkg^{-1})	Growth rate
Africa and Middle East	6.06	4.32	3.4%
Australia and South-East Asia	9.87	4.58	4.6%
China	4.97	2.72	4.6%
Europe	4.36	3.95	2.1%
Eastern North America	4.31	3.79	2.2%
Western North America	4.43	3.92	2.2%
South and Middle America	10.63	7.90	2.9%

Table 3.3: SAF impact metric results for each region with the corresponding growth rate of each region.

Table 3.3 shows a couple of interesting results. Lets first consider the results in the second column. When looking at the SAF impact on a per kg basis, not the Australia and South-East Asia region but the South and Middle America region has the highest value. This is explained by the fact that longer flights consume less fuel per km than shorter flights. As many flights from South and Middle America are relatively long flights going to North America and Europe compared to the shorter flights from Australia to South-East Asia and internal South-East Asia flights, the contrail temperature contribution per kg is higher for the South and Middle America region. So when dividing by the total fuel burn for each region, the South and Middle America region has consumed a lower amount of total fuel compared to the Australia and South-East Asia region, which results in a higher per kg SAF impact.
The third column of Table 3.3 shows the SAF impact metric result when each region has its own individual growth rate. This column shows that a higher growth rate results in a relatively greater reduction in the SAF impact metric. From this it can be concluded that the absolute difference between the baseline kerosene scenario and the ReFuel EU SAF scenario does not grow proportionally with the increase in fuel as a result of the higher growth rate. Therefore, the difference in the SAF impact metric between the South and Middle America region and the Australia and South-East Asia region is even greater in this case due to the much higher growth rate of the Australia and South-East Asia region.
So to give an answer with regards to the initial purpose for this regional analysis, 1 kg of SAF has the greatest impact in reducing the temperature when used in the South and Middle America region.

Now it must be noted that only looking at the region as a whole to determine the greatest SAF impact does not result in the optimal use of SAF. As noted above, a high contrail temperature contribution of a region is a result of having many flights that fly around the equator at cruise altitude and longer flights have a higher per kg SAF impact. This means that the optimal use of SAF is achieved if specifically these flights will use the limited SAF available, regardless of which of the seven regions it belongs to. This is also shown by Teoh et al. (20220) [43], where using a 50% SAF blend distributed to 2% of high warming contrail-flights reduces the RF of contrails by 10%, compared to only 0.6% when using a 1% SAF blend that is uniformly distributed to all flights.

It was discovered during verification that the contrail model of AirClim is not entirely valid for regional analysis. The sum of the contrail temperature contribution of each region is more than the total contrail temperature contribution for the global results. This is only the case for contrails, as all other climate agents do comply with this. A possible reason for this is the fact that the relation between the relative change in RF for contrails with respect to a relative change in particle number emissions of Equation 2.1 is derived from global results only. The effect that this has on the regional results must be investigated in future research.

Finally, for completeness sake, the total temperature contribution split by each climate agent for each region is given in Figure 3.29 until Figure 3.41. For these figures it is interesting to look at the behavior of the CO_2 temperature contribution with respect to the contrail temperature contribution. When

looking at the baseline kerosene graph, for the higher contrail temperature contribution regions, i.e. the Australian and South-East Asian region and the South and Middle American region, the contrail temperature contribution is much higher than the CO_2 temperature contribution for the entire duration of the simulation. For the lower temperature contribution regions, such as the European region, the CO_2 temperature contribution in 2125 even surpasses the contrail temperature contribution. Remember that the regions are divided such that the total number of flown kilometers is approximately equal for all regions. But there are differences in the total fuel burn for each region, which directly relates to the CO_2 emissions. So both the fact that the contrail temperature contribution is different for each region despite their equal number of flown kilometers and the fact that the fuel burn is different for each region, results in this vastly different behavior between the regions of the CO_2 and contrail temperature contribution graphs with respect to one another.

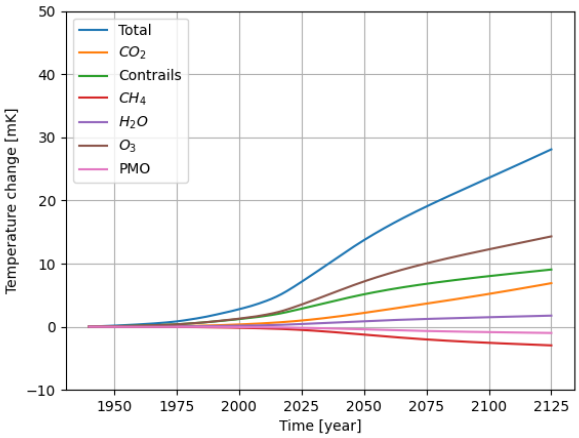

Figure 3.29: Temperature contribution of each climate agent for the baseline kerosene scenario for the African and Middle Eastern region.

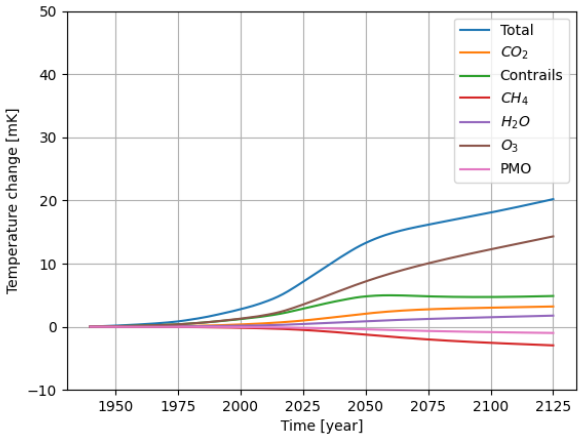

Figure 3.30: Temperature contribution of each climate agent for the ReFuel EU SAF scenario for the African and Middle Eastern region.

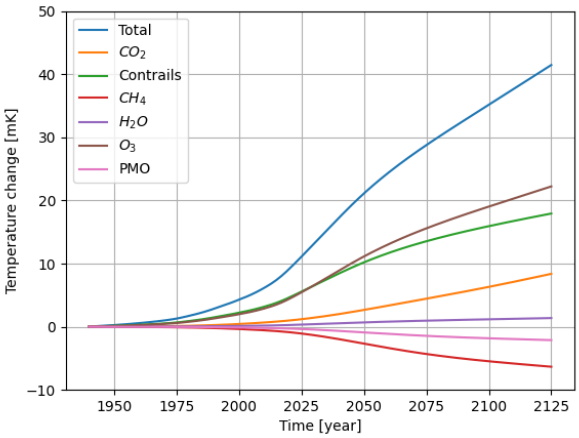

Figure 3.31: Temperature contribution of each climate agent for the baseline kerosene scenario for the Australian and South-East Asian region.

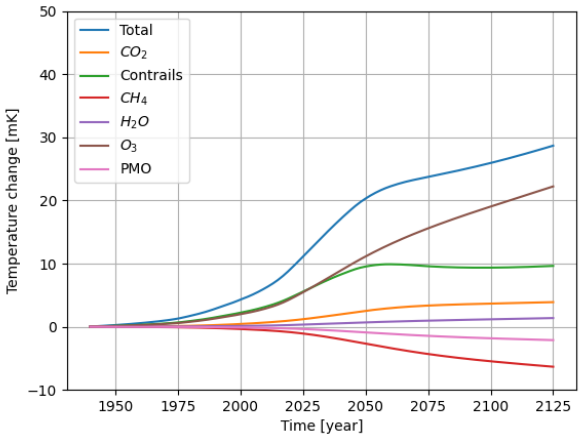

Figure 3.32: Temperature contribution of each climate agent for the ReFuel EU SAF scenario for the Australian and South-East Asian region.

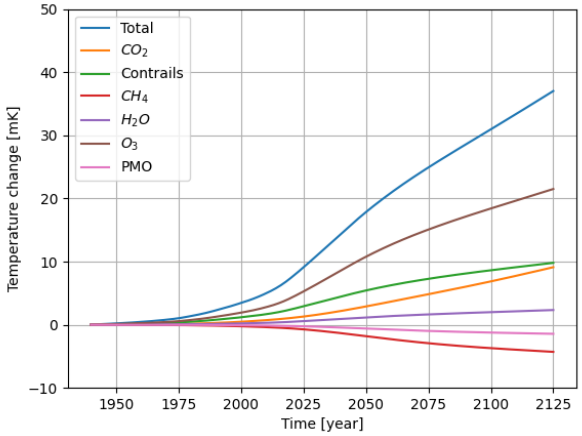

Figure 3.33: Temperature contribution of each climate agent for the baseline kerosene scenario for the Chinese region.

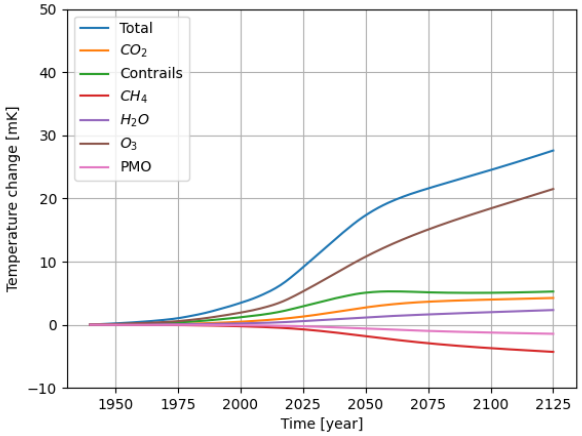

Figure 3.34: Temperature contribution of each climate agent for the ReFuel EU SAF scenario for the Chinese region.

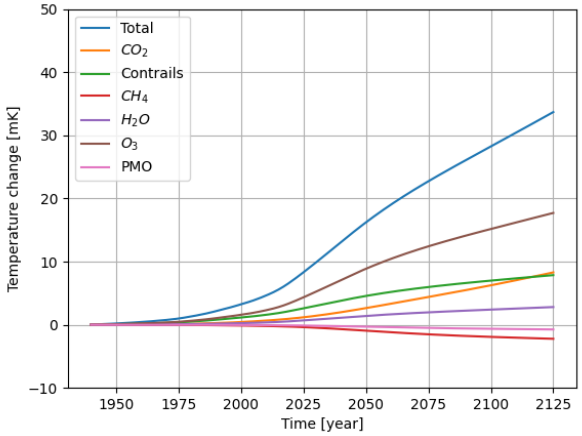

Figure 3.35: Temperature contribution of each climate agent for the baseline kerosene scenario for the European region.

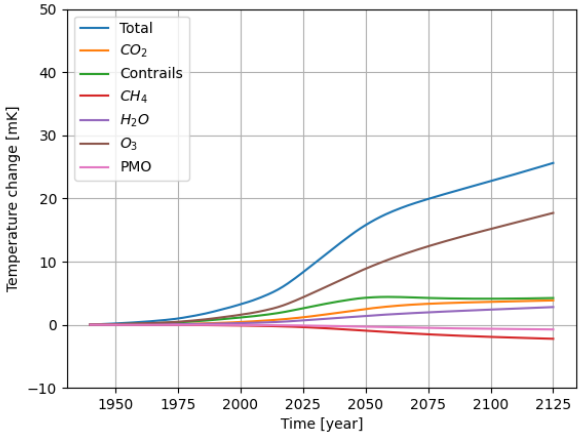

Figure 3.36: Temperature contribution of each climate agent for the ReFuel EU SAF scenario for the European region.

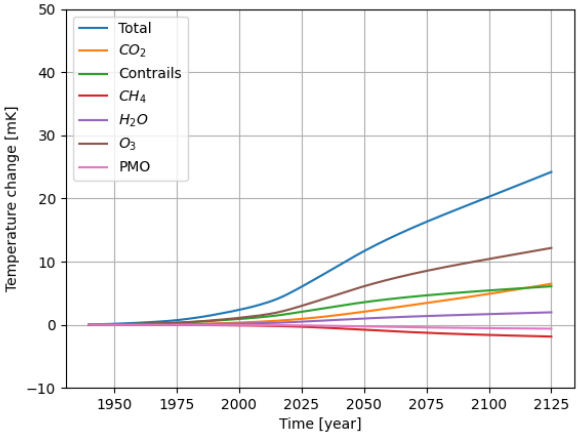

Figure 3.37: Temperature contribution of each climate agent for the baseline kerosene scenario for the Eastern North American region.

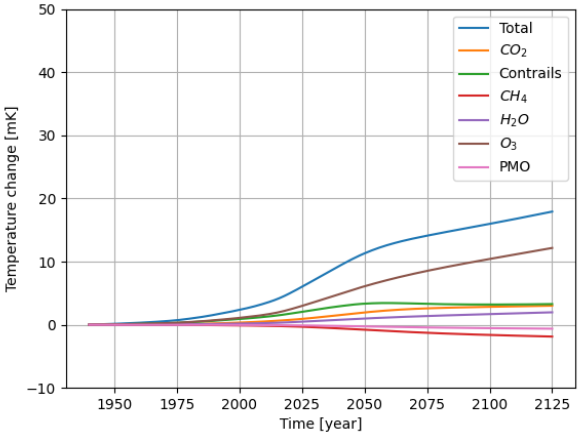

Figure 3.38: Temperature contribution of each climate agent for the ReFuel EU SAF scenario for the Eastern North American region.

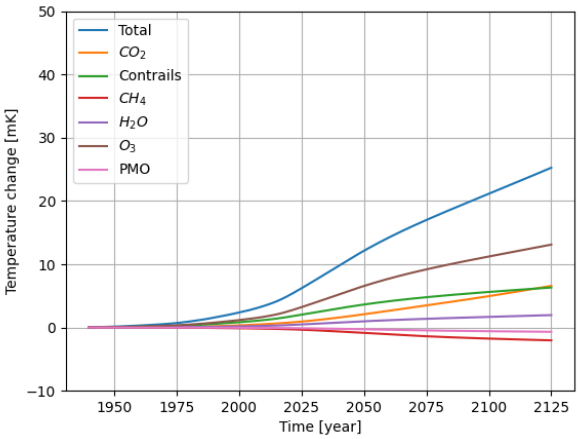

Figure 3.39: Temperature contribution of each climate agent for the baseline kerosene scenario for the Western North American region.

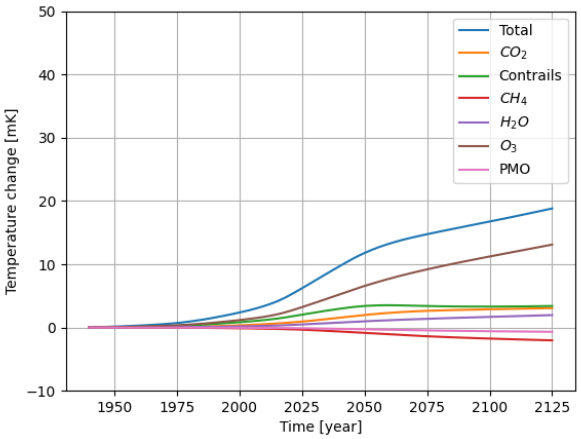

Figure 3.40: Temperature contribution of each climate agent for the ReFuel EU SAF scenario for the Western North American region.

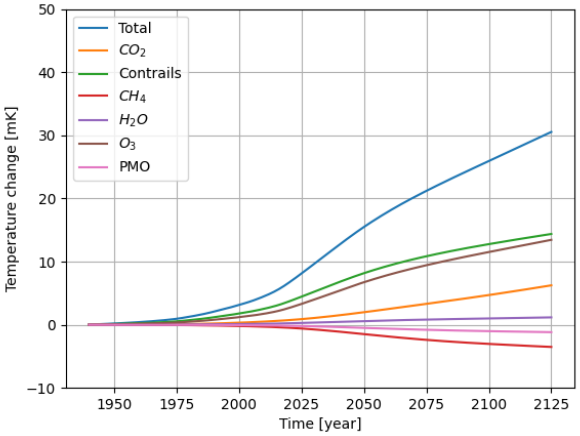

Figure 3.41: Temperature contribution of each climate agent for the baseline kerosene scenario for the South and Middle American region.

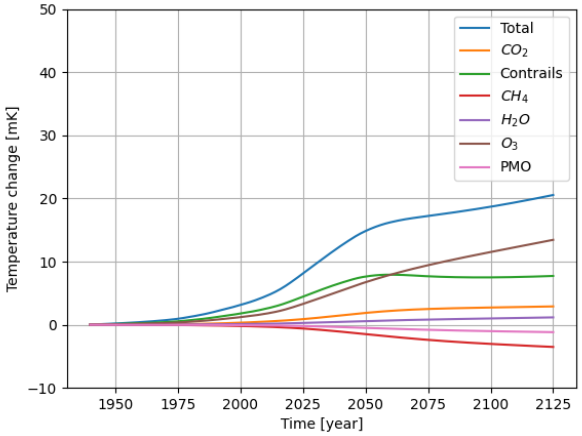

Figure 3.42: Temperature contribution of each climate agent for the ReFuel EU SAF scenario for the South and Middle American region.

Conclusions & Recommendations

The aim of this report was to investigate the impact that sustainable aviation fuels could have in reducing the climate impact of aviation. The research question that lied at the basis of this report was formulated as follows: *How do different scenarios of usage of sustainable aviation fuels, impact the near surface temperature change due to aviation in the year 2125 compared to a baseline kerosene scenario?*.
Below the most important findings from this research will be summarised, which will give an answer to this research question.

The use of SAF (Sustainable Aviation Fuel) has a significant impact in reducing the climate impact of aviation. In 2125 the difference between a SAF usage scenario as imposed by EU legislation (ReFuel EU) and a baseline kerosene scenario is 57.03 mK, meaning a reduction in temperature change of 26.2%.
This scenario still surpasses the Paris Agreement goal of limiting the global temperature rise to 2.0 degrees Celsius by 61.0%. A Monte Carlo simulation shows that for only 6.9% (206 out of 3000 runs), this threshold is not exceeded. This research indicates that, for aviation to accomplish its relative contribution in accordance with the Paris Agreement, an initial overshoot of this goal is almost inevitable. Furthermore, this scenario relies on Power-to-Liquid (PtL), a SAF which uses hydrogen as feedstock and has not yet reached sufficient technological maturity. Without PtL the potential of SAF is reduced, as SAF made from biomass or waste feedstocks has limited scalability due to maximum feedstock availability. In a scenario where PtL does not reach a sufficient technological maturity, the temperature change is only reduced by 26.60 mK (12.2%) compared to the baseline kerosene scenario.

These results show the importance of the non-CO_2 climate agents. Even with the significant use of SAF in the ReFuel EU scenario (resulting in a net 79% CO_2 reduction from 2070 onward), it exceeds the Paris Agreement goal by a significant margin. Especially the unaffected NO_x emissions hurt the climate impact gains that can be achieved. This indicates that efforts to reduce the NO_x emissions are of vital importance. These results also stress the potential for liquid hydrogen powered aircraft in this regard, as that can reduce the NO_x emissions by around 50-80% for gas turbine powered aircraft or 100% for fuel cell propulsion, in addition to completely eliminating the CO_2 emissions.

The background emission scenario that is used for all non-aviation emissions also affects the results. A higher background emission scenario results in a smaller relative and absolute climate impact of aviation, due to the relatively lower aviation emissions when compared to the non-aviation emissions. For a lower background emission scenario the opposite is true. This impact is significant, as the difference in temperature in 2125 between the lowest and highest background emission scenario is 48.91 mK for the kerosene scenario.

The results of a Monte Carlo simulation with 3000 individual runs where 17 parameters were drawn for each run from a uniform distribution, show a large spread. This is a consequence of the large uncertainty ranges (up to $\pm$50%) from which the parameters were drawn. This result emphasises the large uncertainties that are associated with the climate impact of aviation.

Finally, a regional analysis was done to determine the region where the use of 1 kg of SAF would have the highest reduction in temperature compared to the baseline kerosene scenario. The results of this analysis show that 1 kg of SAF can best be used in the South and Middle America region, as it leads to the greatest reduction in temperature. This same result is obtained when each region has their own individual growth rate for Revenue Passenger Kilometer (RPK).

This research has led to a number of recommendations for future studies. These are presented below.

It was found that some discrepancies in the results compared to other studies could be contributed to the emission inventory. It would be advisable to do the same simulations and analyses with emission inventories from similar studies.
This report only focused on the use of SAF as an alternative aviation fuel, but also discusses the potential that liquid hydrogen can have to reduce the climate impact of aviation. A recommendation for further research is to also incorporate liquid hydrogen in these simulations.
For the regional analysis it was discovered during verification that the contrail model is not entirely valid on a regional scale when assessing the climate impact of contrails. This should be addressed for future research.
The regional analysis gives a good indication of how the use of 1 kg of SAF can be optimised and answers the initial question that led to the analysis. However it does not lead to the most optimal SAF usage. This is achieved by specifically identifying high contrail impact flights and ensuring that these flights use the maximum amount of SAF. Further research can be done to identify these specific flights to optimise the use of the limited amount of SAF.

References

[1] Airbus. *Airbus reveals hydrogen-powered zero-emission engine*. 2022. URL: https://www.airbus.com/en/newsroom/press-releases/2022-11-airbus-reveals-hydrogen-powered-zero-emission-engine (visited on 04/04/2023).

[2] Transportation Research Board, Engineering National Academies of Sciences, and Medicine. *State of the Industry Report on Air Quality Emissions from Sustainable Alternative Jet Fuels*. The National Academies Press, 2018. DOI: 10.17226/25095. URL: https://nap.nationalacademies.org/catalog/25095/state-of-the-industry-report-on-air-quality-emissions-from-sustainable-alternative-jet-fuels.

[3] U. Burkhardt, L. Bock, and A. Bier. "Mitigating the contrail cirrus climate impact by reducing aircraft soot number emissions". In: *Clim Atmos Sci* 37 (2018). DOI: https://doi.org/10.1038/s41612-018-0046-4.

[4] Fuel Cells and Hydrogen 2 Joint Undertaking. *Hydrogen-powered aviation : a fact-based study of hydrogen technology, economics, and climate impact by 2050*. Publications Office, 2020. DOI: https://data.europa.eu/doi/10.2843/471510.

[5] N. Chandrasekaran and A. Guha. "Study of Prediction Methods for NOx Emission from Turbofan Engines". In: *Journal of Propulsion and Power* 28.1 (2012). DOI: https://doi.org/10.2514/1.B34245.

[6] *Climate Change 2021 - The Physical Science Basis*. IPCC, 2021.

[7] *Construction begins on world's first integrated commercial plant for producing eFuels*. 2021. URL: https://newsroom.porsche.com/en/2021/company/porsche-construction-begins-commercial-plant-production-co2-neutral-fuel-chile-25683.html (visited on 04/07/2023).

[8] K. Dahlmann et al. "Can we reliably assess climate mitigation options for air traffic scenarios despite large uncertainties in atmospheric processes?" In: *Trans. Res. Part D* 46 (2016), pp. 40–55. DOI: https://doi.org/10.1016/j.trd.2016.03.006.

[9] D. Debney et al. *FlyZero: Zero-Carbon Emission Aircraft Concepts*. Aerospace Technology Institute, 2022.

[10] R.G. Derwent et al. "Global modelling studies of hydrogen and its isotopomers using STOCHEM-CRI: Likely radiative forcing consequences of a future hydrogen economy". In: *International Journal of Hydrogen Energy* 45 (2020), pp. 9211–9221. DOI: https://doi.org/10.1016/j.ijhydene.2020.01.125.

[11] D. DuBois and G. C. Paynter. ""Fuel Flow Method2" for Estimating Aircraft Emissions". In: *SAE Transactions* 115 (2006), pp. 1–14. DOI: http://www.jstor.org/stable/44657657.

[12] EASA. *Introduction to the ICAO Engine Emissions Databank*. ICAO, 2021.

[13] Darren Elliott. *Aviation Fuel Efficiency Technology Assessment*. Tecolote Research, 2015.

[14] Eurocontrol. *EUROCONTROL Data Snapshot*. 2021.

[15] D.W. Fahey and D.S. Lee. "A market based measure for international aviation: need, design, and legal form". In: *Carbon & Climate Law Review* 10.2 (2016), pp. 97–104.

[16] Z. Fan et al. *Hydrogen Leakage: A Potential Risk for the Hydrogen Economy*. Center on Global Energy Policy, 2022.

[17] J.S. Fuglestvedt et al. "Climate effects of NO_x emissions through changes in tropospheric O_3 and CH_4: A global 3-D model study". In: (1997).

[18] *Global Outlook for Air Transport*. IATA, 2023.

[19] V. Grewe, S. Matthes, and K. Dahlmann. "The contribution of aviation NOx emissions to climate change: are we ignoring methodological flaws?" In: *Environmental Research Letters* 14 (2019). DOI: https://doi.org/10.1088/1748-9326/ab5dd7.

[20] V. Grewe and A. Stenke. “AirClim: an efficient tool for climate evaluation of aircraft technology”. In: *Atmospheric Chemistry and Physics* 8 (2008), pp. 4621–4639. DOI: https://doi.org/10.5194/acp-8-4621-2008.

[21] V. Grewe et al. “Evaluating the climate impact of aviation emission scenarios towards the Paris agreement including COVID-19 effects”. In: *Nature Communications* 12 (2021). DOI: https://doi.org/10.1038/s41467-021-24091-y.

[22] M. Howard et al. *FlyZero: the case for the UK to accelerate zero-carbon emissions air travel*. Aerospace Technology Institute, 2022.

[23] C. Hughes et al. *FlyZero: Our Vision For Zero-Carbon Emission Air Travel*. Aerospace Technology Institute, 2022.

[24] IATA. *Sustainable Aviation Fuels: Fact sheet*. 2022. URL: https://www.iata.org/contentassets/ed476ad1a80f4ec7949204e0d9e34a7f/fact-sheet-alternative-fuels.pdf (visited on 04/05/2023).

[25] ICAO. *Carbon Offsetting and Reduction Scheme for International Aviation (CORSIA)*. URL: https://www.icao.int/environmental-protection/CORSIA/Pages/default.aspx (visited on 03/29/2023).

[26] ICAO. *Conversion processes*. 2022. URL: https://www.icao.int/environmental-protection/GFAAF/Pages/conversion-processes.aspx (visited on 04/05/2023).

[27] IEA. *CO2 Emissions in 2022*. International Energy Agency, 2023.

[28] IPCC. “Aviation and the Global Atmosphere”. In: *Cambridge University Press* (1999). DOI: https://www.ipcc.ch/report/aviation-and-the-global-atmosphere-2/.

[29] S. Job et al. *FlyZero: Sustainability Report*. Aerospace Technology Institute, 2022.

[30] B. Kärcher. “Formation and radiative forcing of contrail cirrus”. In: *Nat Commun* 9.1824 (2018). DOI: https://doi.org/10.1038/s41467-018-04068-0.

[31] R. Kroon. “Aviation Emission Inventory: A contemporized bottom-up emission inventory for the year 2019”. In: *TU Delft repository* (2022). DOI: http://resolver.tudelft.nl/uuid:83f7d044-b507-41b6-98de-90f3385c0214.

[32] D.S. Lee et al. “Aviation and global climate change in the 21st century”. In: *Atmospheric Environment* 43 (2009), pp. 3520–3537. DOI: https://doi.org/10.1016/j.atmosenv.2009.04.024.

[33] D.S. Lee et al. “The contribution of global aviation to anthropogenic climate forcing for 2000 to 2018”. In: *AtmosphericEnvironment* (2021). DOI: https://doi.org/10.1016/j.atmosenv.2020.117834.

[34] McKinsey. *Clean Skies for Tomorrow: Delivering on the Global Power-to-Liquid Ambition*. World Economic Forum, 2022.

[35] McKinsey. *Clean Skies for Tomorrow: Sustainable Aviation Fuels as a Pathway to Net-Zero Aviation*. World Economic Forum, 2020.

[36] R. Moore et al. “Biofuel blending reduces particle emissions from aircraft engines at cruise conditions”. In: *Nature* 543 (2017), pp. 411–415. DOI: https://doi.org/10.1038/nature21420.

[37] A. Nuic, D. Poles, and V. Mouillet. “BADA: An advanced aircraft performance model for present and future ATM systems”. In: *Int J. Adapt. Control Signal Process.* 24 (2010), pp. 850–866. DOI: https://doi.org/10.1002/acs.1176.

[38] J. Overton. *An Introduction to Sustainable Aviation Fuels*. 2022. URL: https://www.eesi.org/articles/view/an-introduction-to-sustainable-aviation-fuels (visited on 04/07/2023).

[39] J. Pletzer et al. “The climate impact of hydrogen-powered hypersonic transport”. In: *Atmospheric Chemistry and Physics* 22 (2022), pp. 14323–14354. DOI: https://doi.org/10.5194/acp-22-14323-2022.

[40] A. Skowron et al. “Greater fuel efficiency is potentially preferable to reducing NOx emissions for aviation’s climate impacts”. In: *Nature Communications* 12 (2021). DOI: https://doi.org/10.1038/s41467-020-20771-3.

[41] J. Sun and I. Dedoussi. “Evaluation of Aviation Emissions and Environmental Costs in Europe Using OpenSky and OpenAP”. In: *Engineering Proceedings* 13 (2021). DOI: https://doi.org/10.3390/engproc2021013005.

[42] R. Teoh et al. “A high-resolution Global Aviation emissions Inventory based on ADS-B (GAIA) for 2019–2021”. In: *Preprint* (2023). DOI: https://doi.org/10.5194/egusphere-2023-724.

[43] R. Teoh et al. “Targeted Use of Sustainable Aviation Fuel to Maximize Climate Benefits”. In: *Environmental Science & Technology* 56.23 (2022), pp. 17246–17255. DOI: https://doi.org/10.1021/acs.est.2c05781.

[44] C. Voigt et al. “Cleaner burning aviation fuels can reduce contrail cloudiness”. In: *Communications Earth & Environment* 2 (2021). DOI: https://doi.org/10.1038/s43247-021-00174-y.

[45] *Waypoint 2050*. Air Transport Action Group, 2021.

[46] H. Webber and S. Job. *FlyZero: Primary Energy Source Comparison and Selection*. Aerospace Technology Institute, 2022.

[47] X.S. Zheng and D. Rutherford. *Fuel Burn of New Commercial Jet Aircraft: 1960 to 2019*. ICCT, 2020.